C.P. No. 16
12492
A.R.C Technical Report

MINISTRY OF SUPPLY

AERONAUTICAL RESEARCH COUNCIL
CURRENT PAPERS

Low Speed Tunnel Investigation of the Effect of the Body on C_{m_0} and Aerodynamic Centre of Unswept Wing-Body Combinations

By

A. Anscombe, M.A. and
D. J. Raney, B.Sc.(Eng.), A.C.G I., D I.C.

LONDON: HIS MAJESTY'S STATIONERY OFFICE
1950
Price 5s 6d. net.

C.P. No.16

Report No. Aero.2323

April, 1949

ROYAL AIRCRAFT ESTABLISHMENT

Low-speed Tunnel Investigation of the Effect of the Body on C_{m_0} and Aerodynamic Centre of Unswept Wing-body Combinations

by

A. Anscombe, M.A.
and
D. J. Raney, B.Sc.(Eng.); A.C.G.I.; D.I.C.

SUMMARY

Systematic low-speed tunnel tests have been made on wing-body combinations without tail plane, to find the effect of the body on C_{m_0} and aerodynamic centre position. Model variations included front and rear body length, body diameter, depth and nose shape, wing height and angle, wing root fillet and wing aspect ratio. The wing was not swept back. Dimensions were based primarily on those of current civil aircraft.

The results showed that the change in aerodynamic centre position, K_n, varies linearly with front body length and in a secondary additional way with rear body length; it is virtually independent of wing angle and height. The change in C_{m_0} varies linearly with wing-body angle and roughly with the volume of revolution of the body planform; wing height and fore-and-aft position on the body have only secondary effects. Wing root fillet effects are small on K_n but appreciable on C_{m_0}.

Values of the body effects on K_n and C_{m_0}, calculated by simple impulse theory, were found to agree with the test results in some respects, but to disagree in others. Using this theory as a guide to the correct parameters, semi-empirical formulae have been produced for prediction on other aircraft designs.

The effects calculated by these formulae have been compared with values measured on various wind tunnel models. For the change in K_n, agreement is obtained to within $\pm$ 0.005 in most cases. For the change in C_{m_0}, the formula satisfies the present test results, but badly underestimates most of the ad hoc measurements. Thus, while the prediction of the change in K_n is reasonably satisfactory, some of the C_{m_0} effects still require explanation.

The fillet effects have been analysed as far as possible, but very little work was done and the formulae presented can only be regarded as a stop-gap until further information is available.

LIST OF CONTENTS

		Page
1	Introduction	5
2	Range of tests	5
3	Model details	6
4	Test results and discussion	7
	4.1 Test procedure and presentation of results	7
	4.2 Preliminary test on effect of cabin	8
	4.3 Effect of body and fillets on C_L and $C_{L\ max}$.	8
	4.4 Change in aerodynamic centre position due to body (ΔK_n)	8
	4.41 ΔK_n for bodies of revolution, 9 in. dia., large wing, no fillets	8
	4.42 Effect on ΔK_n of turned-up rear body	9
	4.43 Effect on ΔK_n of altering nose shape	9
	4.44 Effect on ΔK_n of varying body diameter and depth and wing span	9
	4.5 Change in the value of ΔC_{m_0} due to body	10
	4.51 ΔC_{m_0}, for bodies of revolution, 9 in. dia., large wing, no fillets.	10
	4.52 Effect on ΔC_{m_0} of turned-up rear body	11
	4.53 Effect on ΔC_{m_0} of altering nose shape	11
	4.54 Effect on ΔC_{m_0} of varying body diameter and depth and wing span	11
	4.6 Effect of wing root fillets on ΔK_n and ΔC_{m_0}	12
5	Comparison of results with existing methods of estimation	13
	5.1 Existing methods for ΔK_n	13
	5.2 Existing methods for ΔC_{m_0}	14
6	Application of results to prediction on other designs	16
	6.1 Generalisation of the measured ΔK_n (no fillets)	16
	6.2 Generalisation of the measured ΔK_n due to fillets	19
	6.3 Generalisation of the measured ΔC_{m_0} (no fillets)	19
	6.4 Generalisation of the measured ΔC_{m_0} due to fillets	21
7	Summary of methods of prediction	22
8	Conclusions	23
	Notation	25
	References	27

LIST OF APPENDICES

	App.
Potential flow formulae for ΔC_{m_0} and ΔK_n due to body	I
Formula for ΔK_n due to wing root fillets	II
Formula for ΔC_{m_0} due to fillets	III
Accuracy of generalised methods, and comparison with other data	IV

LIST OF TABLES

	Table
Model details	I
Comparison of aircraft dimensions with test model	II
Aerodynamic characteristics of large and small span wings	III
Lift, drag and pitching moment with body for three wing heights	IV
Change in aerodynamic centre and C_{m_0} due to body, no fillets	V
Effect of turning-up rear end of body	VI
Effect of nose-shape variation and cabin	VII
Effect of varying body diameter and depth and wing span	VIII
Change in aerodynamic centre and C_{m_0} due to body, medium fillets	IX
Change in aerodynamic centre and C_{m_0} due to body, small and large fillets	X
Effect of fillet reflex and thickness on $-\Delta K_n$ and $-\Delta C_{m_0}$ due to body	XI
Effect of fillets compared with no-fillet measurements	XII
Analysis of test results on ΔK_n due to body, no fillets	XIII
Analysis of test results on ΔC_{m_0} due to body, no fillets	XIV

LIST OF ILLUSTRATIONS

	Fig.
G.A. of large span wing and 9 in. dia. bodies	1
G.A. of 4.5 in. dia., 9 in. × 13.5 in., and 13.5 in. dia bodies	2
Miscellaneous model details	3
Details of fillets	4
Characteristics of wing alone	5
Lift-effect of wing height and angle, and fillets	6
Pitching moments for range of body front lengths on body rear No.4	7
Forward shift of aerodynamic centre due to body $(-\Delta K_n)$ - no fillets	8
Effect of body size and depth on $-\Delta K_n$, and theoretical values - large wing	9
Effect of body size on $-\Delta K_n$, and theoretical values - small wing	10
$-\Delta C_{m_0}$ due to body - no fillets	11
$-\Delta C_{m_0}$ due to body - no fillets; continued	12

LIST OF ILLUSTRATIONS (Contd.)

	Fig.
Diagram of body forces at $C_L = 0$ for low and high wing	13
Effect of i_w on $-\Delta C_{m_0}$ due to body	14
Effect of body size and depth on $-\Delta C_{m_0}$, and theoretical values - large wing	15
Effect of body size on $-\Delta C_{m_0}$, and theoretical values - small wing	16
Effect of turned-up rear on $-\Delta C_{m_0}$	17
Effect of fillets on aerodynamic centre - normal shape and reflex	18
Effect of fillets on C_{m_0} - normal shape and reflex	19
Effect of fillet reflex and thickness on C_{m_0}	20
Values of Δ_{10} for 9 in. dia. model	21
Charts for estimating ΔK_n due to body of revolution, no fillets	22
Analysis of model results for ΔC_{m_0} due to body	23

1 Introduction

The series of systematic tests described in this report was made to find the effect of the body of an aircraft on the wing aerodynamic centre position and the value of C_{m_0} at low Mach number. The lengths of the bodies tested ahead and aft of the wing were larger, relative to wing chord, than those on which previous empirical rules (Refs.1 and 2) had been based. The main type of aircraft with a long body relative to wing root chord is the transport aircraft with pressurised cabin, and the dimensions of the models tested were based primarily on present-day designs with bodies consisting of a central cylinder of constant diameter, with an elliptic nose fairing, and a rear fairing tapering to a point. In order to make the investigation more complete, the programme was extended to include measurements with a deep body and with a wing of smaller aspect ratio. The effect of wing sweepback was not included in the present investigation: a theoretical treatment of the effect of sweepback on body pitching moment is given in Ref.9.

Some preliminary results have already been given in Ref.3, but these are all included in full here, and the earlier note is now superseded.

This report describes the tests made (Section 4), compares the results with the answers obtained from existing methods of estimation (Section 5) and gives (Section 6) new rules for the prediction of body effects. To facilitate use of the charts, a summary is given in Section 7 of the methods to be used and of their validity as found by comparing with existing model data.

2 Range of tests

Lift, drag and pitching moment were measured over a range of incidence for the following model conditions. No fin, tail plane or nacelles were represented.

(1) Wing alone, aspect ratio = 10 (large span wing) and 5 (small span wing).

(2) With and without cabin on one body length. All further tests made without cabin.

(3) Body of revolution, 9 in. max. dia. Large span wing (A = 10). 4 front and 4 rear lengths;-

Low-wing:- geometric wing-body angles of 0° and 4° ($i_W = 2^\circ, 6^\circ$).

Mid-wing:- geometric wing-body angles of 0° and 4° ($i_W = 2^\circ, 6^\circ$).

High-wing:- geometric wing-body angle of 0° ($i_W = 2^\circ$),

where i_W = angle between body axis and wing no-lift line.
Most of the low wing measurements were made with wing root fillets fitted.

(4) Fillets of various sizes and reflex, tested on low wing, 9 in. dia. bodies.

(5) Turned-up rear body, on low and high wing, several rear body lengths, 9 in. dia. bodies.

(6) Blunter nose fairing, low wing, two front body lengths, 9 in. dia. bodies.

(7) 13.5 in. dia. bodies, mid-wing, two front and two rear lengths.

(8) 4.5 in. dia. bodies, as (7).

(9) 13.5 in. deep × 9 in. wide bodies, as (7).

(10) Small span wing (A = 5) 9 in. dia. bodies, mid-wing, two front and two rear lengths.

(11) Small span wing, 4.5 in. dia. bodies, as (10).

3 Model details

The bodies of maximum diameter 9 in., on which the majority of the tests were made, are detailed in Table I and Fig.1. Comparative dimensions of several transport aircraft, which were used as a basis for the model dimensions, are given in Table II. The models consisted of a straight-tapered wing of mean chord 9.9 in. and with zero sweepback at quarter-chord, and a central cylindrical portion of body of variable length, with end fairings. Both the four front and the four rear body lengths differed from one another by increments of 6.3 in. The nose fairing was a semi-ellipsoid of revolution, and the rear fairing a solid of revolution tapering to a point, typical of the shape found in practice. The same nose and rear fairings were used for all body lengths.

The cabin used for the preliminary test of cabin effect is shown in Fig.3. The body planform was unaltered by the presence of the cabin, and the disturbance in profile in side elevation was moderate, to conform with typical modern full scale design for a large aircraft.

The turned-up rear body is shown in Fig.3. The original body planform was unaltered, and the new side-elevation was obtained by shearing the symmetrical fairing so that the top surface became horizontal.

The 9 in. wide × 13.5 in. deep body models are shown in Fig.2. The planform was the same as for the corresponding 9 in. dia. bodies. The 4.5 in. and 13.5 in. dia. bodies (also shown in Fig.2) were formed by scaling the local diameter of the 9 in. bodies while leaving unaltered the fore-and-aft body dimensions.

Fig.3 shows the small span wing. Except for details in tip shape, this was formed from the large span wing of aspect ratio 10 by halving all spanwise dimensions. The sweepback of the quarter-chord line for the wings was zero, and the section was 18% thick at the centre line and 12% at the tip, with 2% constant camber. The wing sections used, NACA 2418 to 2412, were chosen as having satisfactory characteristics at the Reynolds number of the tests, 0.6×10^6, and are not typical of those used full scale.

Fig.4 shows the wing root fillets tested on the low wing-body combinations. Three sizes were fitted, and these have been labelled "small", "medium" and "large". The size of the fillet likely to be fitted full scale would probably be "small" or "medium". The three sizes were made similar to one another, having equal increments of linear dimension between them. For the majority of the tests - the case called "normal" in the discussion - the fillet upper surface was formed from circular arcs tangential to body and wing surfaces; the variation of arc radius with chordwise station followed a prescribed rule which was the same for all fillets. In the tests where the amount of fillet reflex aft of the wing trailing edge was altered, the fillets were cut and rotated about the wing trailing edge, and the gaps smoothed over with plasticene. The fillet lower surface was flat, and the fillet reflex angle, θ, is defined as the angle between this surface and the no-lift line of the wing. The reflex was (in general) 12° when $i_W = 2$, and 16° when $i_W = 6$ (i.e. the fillet was at the same angle to the body datum). The angle between the wing lower surface near the trailing edge and the no-lift line was about 11°, so the angle between the wing undersurface and fillet undersurface was always small.

Wing-body angle was altered by rotation of the wing relative to body about the line containing the quarter chord point of the wing centre-line chord. Since the wing chord incidence for no-lift was measured as -2°, the two wing-body angles of 0° and 4° at which the tests were made correspond to aerodynamic wing-body angles of 2° and 6°, denoted by the symbol, i_W, and this latter definition has been used throughout the discussion. This is shown diagrammatically in the lower part of Fig.4.

Initially a transition wire was fitted round the body nose fairing but this was removed early in the tests, as it was found that by doing so less scatter was obtained on the pitching moment readings and the mean lines through the points were not appreciably altered.

The tests were made in the No.1 $11\frac{1}{2}$ ft. × $8\frac{1}{2}$ ft. wind tunnel at the R.A.E. between September 1947 and June 1948. The wind speed was 120 ft./sec., which gave a Reynolds number of 0.6×10^6 based on wing mean chord, or 0.85×10^6 based on wing centre-line chord.

4 Test results and discussion

In this section the test results are presented and discussed in relation to the series of systematic tests to which they belong.

4.1 Test procedure and presentation of results

The wing was tested alone at regular intervals throughout the experiment and thus any changes in the datum characteristics could be detected. Such changes were very small. Fig.5 and Table III show the results for typical test runs on the large and small span wings.

The incidence range covered for the majority of the tests corresponded roughly to $C_L = -0.1$ to 0.7, although in some cases readings were taken right up to the stall. Readings were taken at about every $\frac{3}{4}$ deg. over most of the range.

Pitching moments are given about the mean quarter chord point. Coefficients were based on the area and mean chord of the wing planform with the wing continued in straight taper to the body centre-line, since the wing was of this shape when the body was off. This allows the same definitions to be used for all tests independent of body diameter or wing taper. The front and rear body lengths, denoted by the symbols m_o and n_o, are measured relative to the leading edge and trailing edge of this centre-line wing chord, c_o, for the same reason. For purposes of generalisation of the test results, slightly modified definitions of wing area and front and rear body length are stated in section 6 of this report, but no confusion should arise as different symbols have been used when the change in definition occurs; m_o and n_o and c_o are replaced by m, n and c, where c = root chord.

Measurements of C_m for the wing alone were subtracted from the values of C_m for the wing plus body at the same value of C_L in order to obtain ΔC_m due to the body. Some typical $C_m - C_L$ and $\Delta C_m - C_L$ curves are given in Fig.7 to illustrate to what degree the curves are straight; the slope used to define $-\Delta K_n$ due to the body is that at low C_L. The experimental accuracy of $-\Delta K_n$ is about $\pm$ 0.002 for the majority of the tests: in the few cases where some scatter occurred, repetition of measurements did not improve the accuracy.

For the main bulk of the tests, the results are given as $-\Delta C_{m_o}$ and $-\Delta K_n$, the change in pitching moment at no lift and the shift in aerodynamic centre, due to adding the body.

In order to simplify the presentation of the results, the following notation has been adopted:-

Front body lengths are numbered 1, 2, 3 and 4 shortest to longest, and rear body lengths are numbered similarly. This is shown in Table I and Fig.1.

To define a given model combination, the numbers are written down together, front body first; thus, (1, 2) means wing with front body length No.1 and rear body length No.2.

4.2 Preliminary test on effect of cabin

The cabin, illustrated in Fig.3, gave a shift of aerodynamic centre of 0.002$\bar{c}$, destabilising, and changed C_{m_o} by -0.0025. This result is recorded in Table VII. Since these effects were so small, it was decided to make all further tests with the symmetrical body of revolution as nose fairing.

4.3 Effect of body and fillets on C_L and $C_{L\,max}$

In Fig.6 it is seen that wing height has no effect on the lift curve for $i_w = 2^o$ over the range used for the pitching moment measurements. The fillets alter the lift slope slightly. With $i_w = 6^o$, these effects are larger.

The results show no fillet is needed except for the low wing position, and that a larger fillet is needed with the low wing-body angle than with higher angle.

4.4 Change in aerodynamic centre position due to body (ΔK_n)

4.41 ΔK_n for bodies of revolution, 9 in. dia., large span wing, no fillets

This group contains the majority of the tests made.

The aerodynamic centre movement due to body, without fillets, for the three wing heights and two wing-body angles is given in Table V, and plotted in Fig.8 against front body length; this length is expressed as a multiple of wing centre-line chord (c_o = 13.5 in.) in order to give a sense of the model proportions.

In Fig.8 the same two dotted lines are drawn through each set of points, and represent the mean values for all the cases for rear bodies (1) and (4) respectively. It is seen that ΔK_n due to body is practically independent of wing height and wing-body angle. This is supported by the tests with fillets at two wing-body angles (Section 4.6).

Fig.8 also shows that there is a linear relationship between ΔK_n and front body length, the body having a destabilising effect. The rear body length is of much less importance; within the accuracy of the tests this is also linear, and increase in rear body length also destabilises.

The full set of body lengths in the low-wing case was only tested with the "medium" fillets fitted, because some sort of fillet is invariably fitted in actual practice (see Section 4.6).

4.42 Effect on ΔK_n of turned-up rear body (9 in. dia., large span wing)

The effect was found on high wing and on low wing with fillets. The results are given in Table VI. The effect is to cause a numerical reduction in $-\Delta K_n$ of about 0.005, independent of rear body length.

4.43 Effect on ΔK_n of altering nose shape (9 in. dia. body, large span wing)

Table VII gives the results of some brief tests made to compare the standard elliptic nose fairing of length 16.2 in., as used for the majority of the tests, with an appreciably blunter fairing, also elliptic, of length 7.2 in. The nose shapes are compared in Fig.3. The total body-front length remained the same.

The change in $-\Delta K_n$ amounts to 0.009 for the shorter front length (1), and 0.007 for the longer front length (3), the body being more destabilising for the blunter nose fairing than with the normal fairing, for the same overall front body length.

4.44 Effect on ΔK_n of varying body diameter and depth

The 4.5 in. and 13.5 in. dia. and the 9 in. wide × 13.5 in. deep bodies illustrated in Fig.2 were tested with the mid wing at one wing-body angle for two front lengths and two rear lengths. To obtain an accurate overall comparison the corresponding models of 9 in. dia. were tested again at the same time. Similar tests were made on the 4.5 in. and 9 in. bodies using the smaller span wing. The results are compared in Table VIII and plotted in Figs.9 and 10 for the large and small span wings respectively.

The results may be summarised:-

(a) The 9 x 13.5 in. bodies give values of $-\Delta K_n$ which on the average are 7% numerically larger than the corresponding 9 in. dia. body values, showing that increase of body depth has very little overall effect, so that body destabilising depends almost entirely on planform.

(b) ΔK_n varies approximately as $D^{1.6}$ for the range of diameters tested. The ratios are given in Table VIII, which shows they are independent of body length and are the same for both the large and the small span wings.

The effect of wing span is considered further in section 5 below.

4.5 Change in the value of ΔC_{m_0} due to body

4.51 ΔC_{m_0} for bodies of revolution, 9 in. dia., large span wing, no fillets

The change in C_{m_0} due to body without fillets for the three wing heights and two wing-body angles is given in Table 5, and plotted in Fig.11 and 12 against total body length L. This parameter is used rather than front body length (used for graphs of ΔK_n) because front and rear body length are found to be of the same order of importance for ΔC_{m_0}; the length L is plotted as a multiple of wing centre-line chord, c_0. Only a few points with low-wing were obtained without fillets, the full range being tested with fillets (see 4.6).

In Fig.11, where the no-fillet results for the three wing heights are compared at one wing-body angle, $i_W = 2^o$, the points for high wing lie on the graph in a pattern not unlike a parallelogram (except for body (4,4), in which case the point is low). The first short series on the mid-wing (set A) lie fairly well on a line, except for (1,4) and (2,4), which are low. The second short series (set B - made as a check test at a later stage) gave points lying in a narrow parallelogram formation. The two sets are shown superimposed in the lower part of Fig.12. In the case of the low-wing, the few points obtained lie on a straight line except for (3,4) and (4,4), which are low.

There is thus a sequence from low wing to high wing. The straight-line formation of the low-wing series means that ΔC_{m_0} is independent of wing fore-and-aft position of the body. As the wing moves higher up the body, the contribution to ΔC_{m_0} of the rear body becomes less (slope of constant-front-length line decreases) while the contribution of the front body becomes more (slope of constant-rear-length line increases). In all cases the longest rear body, No.4, shows signs of contributing proportionately too little to ΔC_{m_0} compared with shorter rear body lengths. The duality of the results for mid-wing suggests a small degree of instability of the flow over the rear body, as if this is a borderline case between two different regimes of flow.

The effect of wing height on the rear body contribution to ΔC_{m_0} can be explained by reference to the diagrams of Fig.13. In the case of the low wing the wing wake misses the rear body, and as the wing moves from low to high position, the wing wake moves up over the rear body. This is because, at zero lift, the body is nose down. In the high-wing position we may expect the wing wake to decrease the rear body lift by thickening the body boundary layer, and to replace it by an increased drag force. The lift and drag on the front body will not be affected by the position of the wing. The moment arms of the lift forces are independent of wing height, but the drag moment arms depend on wing height, as shown in Fig.13. Thus, on changing from low-wing to high-wing, front body nose-down pitching moment is reinforced due to increase of drag moment arm, while rear body nose-down pitching moment is reduced due to decrease of lift. It is impossible to say what the effect of rear body drag is, as it depends on the length of the moment arm and the amount of drag increase.

The aerodynamic centre was not affected by wing height because the whole contribution of the rear body to ΔK_n is so small that changes would hardly be noticed, while the suggested change in front body drag arm will not appreciably affect ΔK_n if the increase in front body drag with body incidence is small.

The explanation given above is only suggested as satisfying the observed results, and it has not been substantiated experimentally. However, the sensitiveness of the flow over the rear body to disturbing influences in the position of the wing is illustrated by some tests described in Ref.4, where the pitching moment and lift on an inclined torpedo were appreciably different with a thin wire or central spindle suspension.

In Fig.11, the lines joining (1,1) (2,2), (3,3) and (4,4) for high and mid wing (B), and the mean lines through the points for mid wing, set A, and low wing, all lie close to one another. Thus the effects described are relatively small and to a first approximation, ΔC_{m_0} due to body is independent of wing height.

In Fig.12, where the effect of wing-body angle is shown for mid wing, the points at $i_W = 6^o$ form a parallelogram with values closely equal to 3 times the corresponding values at $i_W = 2^o$. This is shown clearly by Fig.14 where some of the values of $-\Delta C_{m_0}$ are cross-plotted against i_W, including the three cases measured with low wing, no fillets.

This indicates that ΔC_{m_0} due to body varies directly with i_W, the angle between body axis and wing no-lift line. This result is supported by the tests described in Ref.17.

4.52 Effect on ΔC_{m_0} of turned-up rear body (9 in. dia., large span wing)

The cases tested with turned-up rear body are compared with the corresponding symmetrical bodies in Table VI and Fig.17. The effect is to decrease $-\Delta C_{m_0}$ numerically. i.e. give a nose-up pitching moment. The change varies from 0.0015 to 0.0085, the value increases with rear body length, and there is a tendency to increase with wing-body angle.

4.53 Effect on ΔC_{m_0} of altering nose shape (9 in. dia. body, large span wing)

On replacing the standard nose fairing by a blunter nose, as described in section 4.43, the negative (nose-down) pitching moment due to body, $-\Delta C_{m_0}$, is numerically increased by 0.0027 for the shorter front body length (1), and by 0.0022 for the longer front length (3).

4.54 Effect on ΔC_{m_0} of varying body diameter and depth and wing span

The 4.5 in. and 13.5 in. dia. and the 9 in. wide × 13.5 in. deep bodies illustrated in Fig.2 were tested with the mid wing at one wing-body angle for two front and two rear lengths. To obtain an accurate comparison, the corresponding models of 9 in. dia. were tested again at the same time. The results are compared in Table VIII and plotted in Fig.15 and 16 for the large and small span wings respectively.

The results may be summarised as follows:-

(a) The 9 × 13.5 in. bodies give values of ΔC_{m_0} on the average 10% larger numerically than the corresponding 9 in. dia. bodies. This shows that increase of body depth has little effect, so that body pitching moment depends mainly on planform.

(b) The effect of body size does not in this case follow a simple power law. The ratios are given in Table VIII. The values for the 9 in. dia. and 4.5 in. dia. bodies are in proportion to $D^{1.6}$ for the large span wing, but for the small span wing the variation is as $D^{1.2}$; the variation between 9 in. and 13.5 in. dia. bodies on the large span wing is in excess of D^2.

The effect of wing span is considered further in section 5.

4.6 Effect of wing root fillets on ΔK_n and ΔC_{m_0} (low wing)

Various tests on wing root fillets were made with low wing, using the 9 in. dia. bodies and large span wing. The measurements can be grouped as follows:-

(1) "Medium" fillets, complete set of front and rear body lengths at two wing-body angles, the inclination of fillet to body being constant (Table IX).

(2) A few tests with "small" and "large" fillets, with various body lengths (Table X).

(3) Effect of altering reflex of "medium" fillets (Table XI).

(4) Effect of varying fillet cross-section (Table XI).

In each case the model had similar fillets in port and starboard wing roots.

The fillets have been described in section 3 and are illustrated in Fig.4. For group (1) above, the fillet lower surface was reflexed at 10° to the body axis for both wing-body angle settings, so that the reflex relative to the wing altered by 4° in changing from $i_w = 2^\circ$ to 6° (reflex angles, θ, $= 12^\circ$ and 16°).

(a) Fillet size - K_n

Fig.18 gives the measurements with medium fillets at two wing-body angles. The mean results without fillets are plotted for comparison. If mean lines are drawn for rear bodies(1) and (4), in the same manner as was done for all the values of $-\Delta K_n$ without fillets on Fig.8, it is seen that the fillet effect is to alter K_n by about 0.015 (stabilising), and that this is independent of body length and wing-body angle.

The individual readings, using the mean values without fillet as datum, are given in Table XII.

In Table XII (but not plotted) are results for the large and small fillets, giving the change in $-\Delta K_n$ as 0.018 and 0.006 respectively. It should be noted that the large fillet was tested in one case only, and that the value obtained is smaller than would be expected. Repeat values without fillet showed some variation, and in this case the mean curve used as zero may not be giving the correct result. This fillet is larger than would be used full scale, and will not be considered further.

(b) Fillet reflex:- K_n

Table XII shows that angle of reflex has no effect on ΔK_n due to fillets.

(c) Fillet thickness:- K_n

Table XII shows that there are increases in K_n when the fillet shape is changed from its normal design, both when it is fattened or reduced to a flat plate coincident with the fillet lower surface. The increases in K_n are respectively 0.008 and 0.018. The changes in fillet shape are illustrated in Fig.4.

(d) Fillet size:- C_{m_0}

Fig.19 shows the measurements of ΔC_{m_0} due to body with small and medium fillets, together with the points for no fillets reproduced from Table V. The one point for large fillets, given in Table X, is omitted. It is seen that, whereas the effect of fillets on K_n is small and independent of reflex, body length and wing-body angle, the effect on C_{m_0} is comparatively large, and varies with body length and wing-body angle. In Fig.19, while the no-fillets case for low wing gave points lying more or less on a straight line, the effect of fillets is to open out the points into a parallelogram formation, as previously noticed for high wing, no fillets (Fig.11). One explanation would be that the addition of fillets causes a disturbance of the flow over the rear body in the same way as was previously suggested for the wing wake if the wing was high on the body; the negative lift in the wing root may also be causing an upwash over the rear body, hence a downward pitching moment proportional to body rear length. The change of C_{m_0} due to fillets is given in Table XII.

The small discrepancies between the "medium" fillet measurements in Tables IX and XI for bodies (1,2) and (1,4) are presumably due to the fillets not being replaced at exactly the same angle in the two series of tests.

(e) Fillet reflex:- C_{m_0}

The results are given in Tables XI and XII and plotted in Fig.20 against angle of reflex relative to wing no-lift line, θ. It can be seen that there is a linear relationship with angle of reflex, and the results are independent of body angle relative to wing.

(f) Fillet thickness:- C_{m_0}

The results are given in Tables XI and XII and are plotted in Fig.20 against θ. It is now apparent that, on the small amount of evidence available, the flat plate points lie on a line passing through $\theta = 0$, while the normal-thickness fillets and fillet-out fillets form a series, showing that fillet thickness, i.e. camber, is a separate parameter to be added to the flat plate results.

An attempt to derive generalised formulae from these results is discussed in section 6.2 and 6.4.

5 Comparison of results with existing methods of estimation

5.1 Existing methods of estimating ΔK_n due to body

An analysis due to Warren (Ref.1) of collected experimental data was based on a comparatively small range of front and rear body lengths, and no attempt could be made from the available results to separate out the effects of body planform, wing aspect ratio or fillets.

The systematic series of tests described in this report has shown that the rear body effect is much smaller numerically than Ref.1 suggested, and has the opposite effect; increase of rear body length increases the destabilising effect to a small degree instead of reducing it. Moreover, it is now seen that ΔK_n due to body is not directly proportional to body width, as Ref.1 supposes.

A purely theoretical approach to the problem was made by Multhopp (Ref.5) and considered in more detail by Schlichting (Ref.6). The method is briefly reviewed, in its application to the present models, in Appendix I. This theory states that in a purely potential field of flow both the front and the rear parts of the body are destabilising, and if there were no curved field of flow due to the circulation round the wing, a geometrically similar front and rear body would produce equal additive effects: however, due to the wing lift, there is an upwash which increases the contribution of the front body, and a downwash which decreases the effect of the rear body. The result is to make the front body the dominating parameter, while the rear body, although still contributing in the same sense, is comparatively unimportant.

The values of ΔK_n due to body are estimated by this theory in Appendix I, and plotted in Fig.9 and 10 in comparison with the test results for the mid-wing models with the three body diameters and two wing aspect ratios. It will be seen that the 9 in. diameter models give measurements in close agreement with the theory - the effect of increase of rear body length is accurately reproduced - but there is bad disagreement for the 4.5 in. and 13.5 in. diameter models. This is because in practice the variation with body diameter followed roughly a $D^{1.6}$ law (see section 4.44), while the potential flow theory gives a D^2 law. It appears, therefore, that the agreement between theory and practice in the case of the 9 in. diameter model is a coincidence.

The theory states that ΔK_n due to body is independent of body depth, and depends entirely on body planform. The results of section 4.44 show that this is nearly borne out in practice.

The small effect noted on turning up the rear end of the body (section 4.42) would not be expected from the theory.

The calculated increases in ΔK_n for the 9 in. diameter bodies on substituting the blunt nose fairing for the standard nose fairing are 0.008 for both front bodies (1) and (3), with the longer front body giving a slightly smaller value than the shorter body. The measured values were 0.009 and 0.007 for the shorter and longer front bodies respectively (see 4.43).

On halving the wing span, $\bar{c}$ is left unchanged, S is halved, the upwash and downwash fields due to wing lift are altered, and the wing lift slope is changed. Carrying out the calculations outlined in Appendix I, the theoretical values ΔK_n due to body for the two wings would be in the ratio 2.7 for all body lengths and diameters. The test results are seen in section 4.44 and Table VIII, to give ratios varying between 2.3 and 2.5.

There is no existing theory or analysis of fillet effects with which to compare the present model data.

5.2 Existing methods of estimating ΔC_{m_0} due to body

The analysis due to Haile (Ref.2) separated the low, mid and high wing cases into three different empirical relationships. The data used in the analysis suffered, as in Ref.1, from the smallness of the range of body length, and a miscellaneous array of body sizes and fillets.

The results of the present systematic tests have shown that wing height is not an important variable so long as fillets are not fitted (Section 4.51) and that fillet effects may be considerable and should be considered as a separate variable (Section 4.6). The results now obtained without fillets lie to a first approximation about 50% above the line given in Ref.2 for mid-wing.

The theoretical analysis of Ref.5 and 6 already described in Section 5.1 and outlined in Appendix I gives the result:-

$$\Delta C_{m_0} = -\frac{2\, i_w}{S\bar{c}} \cdot \text{Vol},$$

i_w being in radians, where Vol. is the volume of the solid of revolution having the same planform as the body. The result is independent of wing fore-and-aft position on the body.

The values of ΔC_{m_0} due to body are estimated by this formula in Appendix I and are plotted in Fig.15 and 16 in comparison with the test results for the mid-wing models with the three body diameters and two wing aspect ratios. It will be seen that the experimental results for the 9 in. and 13.5 in. diameter models lie well below the theoretical, being only about 0.5 of the estimated values. The experimental results for the 4.5 in. bodies agree more nearly with the theory (factor about 0.7). The amount of the discrepancy varies because the theoretical values follow a D^2 law, inherent in the volume term, while the experimental values do not. The theoretical formula gives points all lying on a single straight line, independent of wing fore-and-aft position, while the experimental values only approximate closely to a straight line law for the case of the low wing (Fig.11).

The theory states that ΔC_{m_0} due to body is independent of body depth, and depends entirely on body planform. The results of section 4.54 show that this is approximately borne out in practice.

The small effect noted in the experiments on turning up the rear end of the body is not covered by the theory, which only considers a long straight body.

The calculated change in ΔC_{m_0} on substituting the blunt nose for the normal longer nose is -0.0041. The measured values (see Section 4.53) are still related to the calculated by the factor of about 0.5 noted already for the whole ΔC_{m_0} due to body for 9 in. diameter models.

The theory states a direct proportionality to aerodynamic wing-body angle, i_w. It was shown in Section 4.51 and Fig.14 that this was in fact true in practice.

On halving the wing span, $\bar{c}$ is left unchanged and S is halved, so that theoretically the values of ΔC_{m_0} due to body are exactly doubled. The experimental values (Section 4.54 and Table VIII) give a multiple varying between 1.9 and 2.8, with a mean value of 2.2.

There is no existing theory or analysis of fillet effects with which to compare the present model data.

6 Application of the results to prediction for other designs

Up to now we have been concerned purely with the results obtained in the present series of systematic tests. An attempt is now made to generalise the results in a non-dimensional form suitable for the prediction of body effects on other aircraft designs.

In Section 5 it was shown that the simple potential flow formulae of Ref.5 and 6 are in some respects supported closely by experiment, but in other respects, notably the variation with body diameter, the theory needs modification. Therefore, in the following analysis, the potential flow theory has been used as a basis where convenient and empirical curves have been derived to tie up theory and experiment.

Finally, charts are given for prediction purposes in Figs.22 and 23. Previous ad hoc experimental results are compared in Appendix IV with the values estimated by the methods derived here, for a number of aircraft models. There have not been many suitable tests made, and more data would be valuable, especially on fillet effects.

The methods of prediction derived here are summarised in Section 7.

6.1 Generalisation of the measured ΔK_n due to body (no fillets)

As explained in Appendix I, a simple theoretical value of ΔK_n due to body can be obtained from Ref.5 and 6 in the form

$$\Delta K_n \propto \frac{-cD^2}{aS\bar{c}}\left[\left(\frac{m}{c}\right)\left(\frac{d\beta}{d\alpha}\right) - (\text{nose taper effect}) + (\text{rear body effect})\right]$$

The second and third terms are both small compared with the first; the second term is nearly independent of $\frac{m}{c}$, while the third term is completely independent. This theoretical expression has been used as a basis of the present analysis.

It was seen in Fig.8 that mean values of ΔK_n could be taken independently of wing-body angle and wing height, with no appreciable loss of accuracy. These mean values for the 9 in. diameter bodies, and the mid-wing values for the 4.5 in. and 13.5 in. diameter bodies - all without fillets, and on the large span wing of aspect ratio 10 - have been expressed in a form suggested by the theoretical formula quoted above:-

$$\Delta_{10} = -\Delta K_n \cdot \frac{aS\bar{c}}{cD^2} .$$

The values of Δ_{10} are given in Table XIII for the three body diameters, and the values for the 9 in. diameter bodies only are plotted in Fig.21 against front body length expressed as $\frac{m}{c}$.*

The ratios, k, of the values of Δ_{10} for 13.5 in. and 4.5 in. diameter bodies to the corresponding 9 in. diameter bodies, are also given in Table XIII, and it will be seen that, within the accuracy to be expected from the original measurements, the values of k are independent of body length.

This analysis is repeated in the same Table for the results on the small aspect ratio wing ($A = 5$). The values of Δ for $A = 5$ are written Δ_5.

It is now possible to plot in Fig.22 (lower right-hand side) the factor, k, which correlates empirically the variations with body diameter ratio, D/c. It is necessary to treat body diameter in a non-dimensional form, and root chord c has been chosen for convenience. The factor k is seen to be independent of wing aspect ratio.

At the foot of Table XIII, the results for the two wing spans are compared in the ratio $\frac{\Delta_5}{\Delta_{10}}$. This ratio is seen to be practically the same for all body lengths. In the lower left-hand part of Fig.22, the values of the ratio are plotted against wing aspect ratio A. The dotted line shown is the theoretical relationship connecting Δ_A, for any aspect ratio, and Δ_{10}, and gives us a guide to the correct curve connecting the points for $A = 5$ and $A = 10$, so that the experimental results can be presented in the generalised form $\frac{\Delta_A}{\Delta_{10}}$.

In order to complete the generalisation of the results, a modified version of Fig.21 is derived as follows:-

The curves of Fig.21 cannot be produced indefinitely towards the origin without modification because the nose of the body tested was rounded off elliptically throughout the first 16.2 in. of its length; this is equivalent to $\frac{m}{c} = 1.26$ (the actual value varies slightly with small changes in c for various wing-body combinations). Obviously the existing curves of Fig.21 must be modified for $\frac{m}{c} < 1.26$, because shorter front body lengths must have shorter nose fairings. We may

* The values of c, m and n used throughout Section 6 are derived by letting the intersection of wing leading and trailing edges with the body planform define the root chord c. The wing planform is taken as rectangular inside the body, and is not considered to taper to a maximum value, c_0, on the body centre-line, as was used in the previous parts of the report. Throughout the presentation of the results in the report this latter definition of wing area was used, as it would have been extremely confusing in comparing answers if the units changed with body diameter and wing aspect ratio, but in applying the generalised results to other aircraft designs it is likely to prove much simpler and more logical to use the definitions, based on root chord, now suggested. It is also considered that the upwash and downwash fields which control the pitching moments on the body must be functions of the wing planform outside the body only.

The values of c, m and n, which now replace c_0, m_0 and n_0 as definitions of body length, vary slightly with body diameter and wing aspect ratio. They are listed fully in Table I. The values of Δ_{10} and Δ_5 are of course derived from the measured ΔK_n, which was based on $S\bar{c}$ of the fully tapered wing, by using the early definition of S and $\bar{c}$. The new definitions are illustrated by the diagrams in Fig.21 and 22.

safely assume that the whole of any front body length with $\frac{m}{c} < 1.26$ consists entirely of nose fairing; the error involved is likely to be very small. It was seen (Section 4.43) that, when the length of the curved part was shortened from $\frac{m}{c} = 1.26$ (i.e. m = 16.2 in.) to $\frac{m}{c} = 0.56$ (the equivalent of 7.2 in.), the total front body length being unaltered, then the mean change in ΔK_n on the 9 in. diameter bodies was 0.008. This in terms of Δ_{10} is equivalent to 0.35. Hence, in Fig.21, the position of the lines at $\frac{m}{c} = 0.56$ is obtained by extrapolation of the present lines down to this point, with an addition of 0.35 to the corresponding values of Δ_{10}. This gives sufficient guide for drawing the curve for low $\frac{m}{c}$. The required extrapolation is shown by the dotted line of Fig.21.

A similar trouble arises for values of $\frac{n}{c}$ less than 2.1, because the last 27 in. of the models formed a fairing tapering to a point. Rear body lengths shorter than this would have to be blunter. We have no experimental measurements to use, but since the theory of Ref.5 was seen in Section 5.1 to give a good estimate of rear body effects on the 9 in. diameter bodies, we can use the calculated values with sufficient accuracy to obtain the lines of Δ_{10} for $\frac{n}{c} = 1$ and $\frac{n}{c} = 0$.

The upper half of Fig.22 shows the values of Δ_{10} for the 9 in. diameter bodies replotted in chart form suitable for general use. The actual experimental values of $\frac{n}{c}$ have been replaced by round numbers to facilitate use of the chart.

Summarising, the calculated value of ΔK_n due to a body of revolution is given by

$$\Delta K_n = -\Delta_{10} \cdot \left(\frac{\Delta_A}{\Delta_{10}}\right) \cdot k \cdot \frac{cD^2}{a S\bar{c}} \qquad (1)$$

where Δ_{10}, $\left(\frac{\Delta_A}{\Delta_{10}}\right)$ and k are read off the curves of Fig.22, "c" is the root chord, at the junction of wing and body, "a" is the lift slope per radian, and D, it is suggested, is taken as the body diameter (or width) at the position of the wing leading edge; because, in the case of the body which does not have a constant diameter, the value of D should refer to front body rather than rear body since rear body effects on ΔK_n are of a secondary order.

The other variables in body shape not yet considered are:-

(a) Body depth. The results of 4.44 suggest that 7% might be added to ΔK_n for round bodies, if the depth is increased by 50%. Hence the rule

$$\Delta K_n = \left[\text{round body value of equation (1)}\right] \times \left[1 + 0.15\ \frac{(h-D)}{D}\right] \qquad (2)$$

where $\frac{h}{D}$ = body $\frac{\text{depth}}{\text{width}}$ ratio.

(b) Cabin. The effect was negligible for the shape tested. (Section 4.2).

(c) Turned-up rear body. In 4.42 it was seen that $-\Delta K_n$ due to body was decreased by 0.005 for any body length. This can now be generalised by making this equivalent to a decrease in Δ_{10} of 0.22 for a fully turned-up rear. The effect is small, and an intermediate degree of sweep-up could be dealt with by interpolation.

(d) Different body nose planform. Blunter noses have already been considered; the changes described in Section 4.43 only resulted in a very small change in K_n due to body. It was seen in Section 5.1 that the potential flow theory of Ref.5 and 6 gave this small change closely and, indeed, the theory agreed quite well with the model values of ΔK_n for the one case of the 9 in. diameter bodies on the large span wing. This useful result suggests that the effect of a very different nose-shape e.g. the long pointed cone of a supersonic body, could be calculated with sufficient accuracy by the method outlined in Appendix I so long as the result is applied in the form Δ_{10} so as to make it subject to the empirical rules for body diameter and wing aspect ratio variations.

(e) Different body rear planform. The contribution of the rear body to K_n is so small that we can safely ignore differences in rear body planform.

6.2 Generalisation of the measured ΔK_n due to fillets

The test results of 4.6 showed that the fillet effect is small and is independent of wing-body angle, angle of reflex and body length. It is therefore basically a function of planform geometry of the wing, body and fillet. If we consider the fillet to act as a rearward extension of the wing, and assume the effect to be carried right through the wing, an approximate expression can be calculated for the rearward shift of the wing mean quarter chord point. The calculation is given in Appendix II. This formula is seen in Appendix IV to agree satisfactorily with the systematic test model results for the "small" and "medium" fillets, but breaks down for the one test result with "large" fillets.

The test results with flat plate and extra-thick fillet do not give enough information to make any generalisations about the effect of fillet thickness. Quite possibly the effect observed with the flat plate fillet was due in part to a wake from the wing-body junction affecting the flow over the rear part of the body.

6.3 Generalisation of the measured ΔC_{m_0} due to body - no fillets

Since, for all bodies without fillets, there was no measurable change of zero lift angle compared with the wing alone, the wing itself is at zero lift when we are measuring ΔC_{m_0} due to body. Therefore the only effects the wing can have are interference effects due to the velocity increment round the wing (likely to be negligible) and due to the wake and distortion of the flow over the rear part of the body. This latter could be observed when low-, mid- and high-wing combinations were compared in Section 4.51. There was an effect which varied with wing height, but the differences in the value of ΔC_{m_0} for a given body front and rear length were quite small. The fifth column of Table XIV gives the mean values of $-\Delta C_{m_0}$ for $i_w = 2^o$ for the three wing heights on the bodies of revolution. The greatest error in taking a mean is only 0.004 in the worst case, and most of the original values are much closer to the mean than this.

Apart from the interference of the wing on the body at $C_L = 0$, the only parameters controlling the results must be the dimensions of the bodies themselves. In order, therefore, to present the values of ΔC_{m_0} in a form independent of wing dimensions, and since we know they are proportional to i_w, the function f has been tabulated in the last two columns of Table XIV where

$$f = (-\Delta C_{m_0}) \times \frac{S\bar{c}}{\text{Vol.}i_w}$$

where Vol. = volume of body of revolution.

This form was suggested by the theoretical values for ΔC_{m_0} (see Appendix I). We have omitted consideration, for the time being, of the deep bodies tested or the bodies with turned-up rear part, and of the wing root fillets.

The values of f for the three body diameters, the two wing-body angles and the two wing aspect ratios have been plotted in Fig.23 against the body fineness ratio L/D where L = total length of body and D = body maximum diameter.

It will be seen that the three diameters form a series giving values of f which increase with L/D. For the 9 in. diameter bodies the points with wing aspect ratio A = 5 lie a little below those for A = 10, while on the 4.5 in. diameter bodies the reverse is the case. It can therefore be concluded that wing aspect ratio has no predictable effect. The points for the 4.5 in. bodies are rather scattered, but the volume is smallest for this case and therefore experimental scatter shows up most here. The lines in Fig.23 join points with constant N/D, where N is the rear body length measured from the wing quarter chord point. This is chosen as the point of reference for rear body length because the wing affects the pitching moment on the body only by distorting the flow over the rear body. It would therefore be wrong to express rear body length as the distance, n, from wing trailing edge, since this would erroneously bring the numerical dimensions of the wing chord into the analysis.

It is seen in Fig.23 that the values of N/D increase fairly consistently from left to right across the graph.

The physical interpretation seems to be that, the greater the body fineness ratio L/D, the nearer the actual values of $-\Delta C_{m_0}$ due to body approach the theoretical[5] value in potential flow of $\dfrac{2\ \text{Vol.}\ i_w}{57.3 \times S\bar{c}}$, which is equivalent to $f = \dfrac{2}{57.3} = 0.035$. Also, for a given overall length of body, the larger the rear body arm N the more the measured value of ΔC_{m_0} falls below the theoretical.

This variation with N, i.e. with point of reference of pitching moment, is not large, and the variations observed in Fig.23 due to change of wing-body angle or aspect ratio, are nearly of the same order of magnitude. Therefore a single line as drawn in Fig.23 seems a sufficiently accurate generalisation.

$$\text{Thus } \Delta C_{m_0} \text{ due to body} = -f \cdot \frac{\text{Vol.}\ i_w}{S\bar{c}} \qquad (3)$$

where f is read from the straight line of Fig.23.

Comparison with available ad hoc data is made in Appendix IV where it is seen that this generalisation underestimates in most cases considered.

The fact that there is an apparent small variation with N/D in Fig.23 for a given L/D might need further consideration in the case of aircraft with highly swept back wings, because the question arises as to whether N is being measured from the C.G. or from the wing root quarter chord point (which were coincident on the systematic test model).

The other body variables covered by the present series of tests are:-

(a) Body depth. The results of Section 4.54 suggest a rule to add 10% to the values estimated for bodies of revolution if the depth is 1.5 times the width.

This gives the formula

$$\Delta C_{m_0} = \left[\text{round body value from equation (3)}\right] \times \left[1 + 0.2\left(\frac{h-D}{D}\right)\right] \qquad (4)$$

where $\frac{h}{D}$ = body $\frac{\text{depth}}{\text{width}}$ ratio.

(b) Cabin. The effect of the cabin tested (Section 4.2) was very small. Further experimental values are available in Ref.7.

(c) Turned-up rear body. The measured values (Section 4.52) suffer from experimental scatter. Comparison of the change in C_{m_0} due to turning up the rear body, with the corresponding no-fillet values of ΔC_{m_0} due to body suggests that the effect could be represented by reducing $-\Delta C_{m_0}$ numerically by one fifth. The effect is small and the rule seems sufficiently accurate, even if it has no physical foundation.

(d) Body nose variations. As discussed in 5.2, the effect of nose shape variations follows the same rule as that of the whole body, both being related to the potential flow estimate by the same empirical factor. Hence the charts of Fig.23 automatically include any nose shape variation (symmetrical) in the volume of revolution. No data are available on the effect of turned-up or turned-down nose fairings.

(e) Different rear body planform. On the evidence of the paragraph above all rear planforms are included in the volume.

6.4 Generalisation of the measured ΔC_{m_0} due to fillets

Fig.20 showed that the fillet effect consisted of a flat plate effect varying linearly with angle of deflection relative to wing no-lift line, together with a thickness term of opposite sign, which was constant for all angles of deflection, and varied with fillet upper surface shape.

It is seen in Appendix III that the flat plate results are larger than those which would be expected from a plain flap in the position of the body and fillets. By writing the plain flap estimate in a generalised form and connecting it with the test results by empirical factors, a formula has been derived which satisfies the model results (except for the one case tested with "large" fillets), but is not supported by the few other test results available.

7 Summary of methods of prediction (List of notation given elsewhere)

7.1 ΔK_n due to body (no fillets)

For body of revolution, $$\Delta K_n = -\Delta_{10} \cdot \left(\frac{\Delta_A}{\Delta_{10}}\right) \cdot k \cdot \frac{cD^2}{aS\bar{c}} \qquad (1)$$

body destabilising, where Δ_{10}, $\frac{\Delta_A}{\Delta_{10}}$ and k are given in Fig.22, and require a knowledge of front and rear body overhang, m/c and n/c, body diameter ratio D/c, and wing aspect ratio. D is taken as body width at wing L.E., a = lift slope per radian. For a deep body,

$$\Delta K_n = \left[\text{round body value from (1)}\right] \times \left[1 + 0.15\left(\frac{h-D}{D}\right)\right] \qquad (2)$$

where $\frac{h}{D}$ = body $\frac{\text{depth}}{\text{width}}$ ratio.

For a fully turned-up rear end to the body (i.e. tapering to a point on level of body upper surface), subtract 0.22 from Δ_{10}.

For a very different nose shape from that used in the tests of this report, the value of Δ_{10} can be calculated by the method of Appendix I, and the empirical values of $\frac{\Delta_A}{\Delta_{10}}$ and k applied from Fig.22.

For a different rear shape, no correction need be made. Appendix IV shows good agreement with ad hoc test results, to ± 0.005 on ΔK_n in most cases.

7.2 ΔK_n due to fillets

Formula suggested is

$$\Delta K_n = \frac{\ell_f(c + \ell_f)(D + b_f)}{4S\bar{c}} \qquad (3)$$

where ℓ_f and b_f are the maximum length and breadth of the fillet outside body and wing as seen in planform outline. Fillets are stabilising.

This holds for small and medium sizes of systematic test fillet, but the two ad hoc results available do not agree.

7.3 C_{m_0} due to body, no fillets

For body of revolution,

$$\Delta C_{m_0} = -\frac{f.\text{Vol}.i_w}{S\bar{c}} \qquad (4)$$

being a nose-down pitching moment for normal wing-body angles. The factor f is read off Fig.23, requiring a knowledge of body fineness ratio L/D. For a deep body,

$$\Delta C_{m_0} = \left[\text{round body value from (4)}\right] \times \left[1 + 0.2\left(\frac{h-D}{D}\right)\right] \qquad (5)$$

where $\frac{h}{D}$ = body $\frac{\text{depth}}{\text{width}}$ ratio.

For a fully turned-up rear body, ΔC_{m_0} is numerically decreased by one-fifth of the round-body value.

Any nose and rear fairing shapes on bodies of revolution are included in equation (4) in the volume of body.

Although these formulae are satisfied by the results of the present series of systematic tests, ΔC_{m_0} is badly underestimated numerically for most of the ad hoc test results investigated, the estimate being a half to two thirds of the measured value, i.e. 0.01 or 0.02 too low.

7.4 ΔC_{m_0} due to fillets

The formula derived in Appendix III is

$$\Delta C_{m_0} = \left[\left(0.046 + 0.08 \frac{dC_m}{dC_L}\right) \lambda_1 \theta - 0.2 \frac{(c + \ell_f)}{c}\right] \frac{(D + b_f)}{b} ,$$

the first term being due to the reflex of the fillet lower surface, the second term being the effect of fillet upper surface shape.

This fits the small and medium fillets tested, but needs more experimental evidence before it can be substantiated.

7.5 Effect of cabin

The cabin tested had negligible effect on ΔK_n: it is probably satisfactory to ignore the cabin in general. ΔC_{m_0} was increased numerically very slightly by addition of the cabin; other data are available in Ref.7.

8 Conclusions

The model tests described here have covered the case of a body on a tapered wing without sweepback. The changes in aerodynamic centre position, K_n, and in C_{m_0}, due to body, have been found for a range of body front and rear lengths, nose shape, body width and depth, wing-body angle and height. and wing aspect ratio. The results may be summarised:-

(1) The main parameters affecting change in aerodynamic centre position due to body are body front length and width; rear length has a secondary added effect. It is practically independent of body depth, wing-body angle and wing height. The front length variation is linear and the width variation lies between a linear and a square law. Charts have been constructed which incorporate non-dimensionally the effects of the various parameters with good accuracy. On comparing estimates based on these charts with results obtained in other ad hoc model tests it is found that the agreement is within about ± 0.005 on K_n in most of the cases tried, the worst discrepancy being 0.024.

(2) The change in C_{m_0} due to body varies linearly with the angle between wing no-lift line and body axis, and the variation with body width is more scattered, but of the same type as for the changes of K_n. The effect of wing height is small. The variations with body front and rear length are complicated. Charts have been constructed which reproduce non-dimensionally the present test results with good accuracy. It is found that estimates based on these charts for other aircraft designs give good agreement with model results in a few of the cases examined, but badly underestimate in most, the discrepancy being of the order of

0.01 or 0.02. The lack of more consistent agreement may be due to difficulties in the definition of body axis in some cases, or to the effects of large cabins.

(3) Tests made with wing root fillets of various sizes, reflex angles and thickness, show that the effect on aerodynamic centre is small, but the effect on C_{m_0} may be considerable. Semi-empirical formulae have been derived connecting the observed variations, but more work is necessary for a full understanding of fillet effects. The suggested formulae which are based on the systematic model test results, are not supported by the few ad hoc results available.

NOTATION

A = wing aspect ratio

a = lift slope of wing or wing plus body, per radian

b = wing span; also used as local body width in Appendices

b_f = span of fillet measured from edge of body in plan view to junction with wing T.E.

c = root wing chord, at junction of wing and body planform

c_o = wing centre-line chord when wing is tapered to centre line

$\bar{c}$ = wing mean chord

C_L = wing or wing plus body lift coefficient

C_m = wing or wing plus body pitching moment, measured during tests about mean $\frac{1}{4}$ chord point

C_{m_o} = C_m at zero lift

ΔC_{m_o} = change in C_{m_o} due to body or fillets

D = maximum body diameter of test models

= body width at wing L.E. in generalised analysis of ΔK_n due to body

f = $-\Delta C_{m_o} \times \dfrac{S\bar{c}}{\text{Vol } i_w}$, i_w in degrees

h = body depth

i_w = aerodynamic wing-body angle, measured in degrees unless otherwise stated

= angle between no-lift line of wing, and body axis

K_n = position of aerodynamic centre of wing or wing plus body, relative to L.E. of mean chord as a factor of $\bar{c}$

$$= 0.25 - \left(\frac{dC_m}{dC_L}\right)$$

ΔK_n = change in aerodynamic centre position due to addition of body or fillets to wing. Positive for stabilising change.

k = factor connecting ΔK_n for various body diameters

L = total body length

ℓ_f = chord of fillet measured from wing root chord T.E. to junction of fillet and body planforms

M = overall moment on inclined body in field of potential flow

m = body front length ahead of L.E. of wing root chord, c.

m_0 = body front length ahead of L.E. of wing centre-line chord , c_0

N = body rear length aft of wing root quarter chord point

n = body rear length aft of T.E. of wing root chord, c

n_0 = body rear length aft of T.E. of wing centre-line chord, c_0

S = wing area taken as area of wing tapered to centre line in presentation of results, or defined as preferred in application of general analysis

V = velocity of free stream

Vol = volume of revolution of the body plan form = true volume for body of revolution

α = incidence of wing chord line to free stream

β' = local angle of inclination of air to body

Δ $= \Delta_A = \left(-\Delta K_n\right) \dfrac{aS\bar{c}}{cD^2}$ for wing of any aspect ratio

Δ_{10} = value of Δ when wing aspect ratio = 10

Δ_5 = value of Δ when wing aspect ratio = 5

ε = downwash angle behind wing at position of body centre-line

θ = angle, in degrees, of reflex of fillet lower surface to wing no-lift line

$\overline{\dfrac{d\beta}{d\alpha}}$ = mean value of $\dfrac{d\beta}{d\alpha}$ from a given position ahead of wing down to wing L.E.

LIST OF REFERENCES

No.	Author	Title, etc.
1	Warren	A method of estimating the forward shift of neutral point due to body shapes, deduced from wind tunnel tests. ARC 8071. RAE Report No. Aero.1960 (August, 1944). (Unpublished)
2	Haile and Piper	Note on the estimation of C_{m_0}. ARC 6075. RAE Report No. Aero.1743 (July, 1943). (Unpublished)
3	Anscombe and Tatchell	Preliminary results of wind tunnel tests on effect of a long cylindrical fuselage on longitudinal stability. ARC 11,664. RAE Technical Note No. Aero.1930 (January, 1948). (Unpublished)
4	Albring	Applicability of the results of wind tunnel measurements on solids of revolution to full scale conditions. German Document Centre 10/1462 (1944). (Unpublished)
5	Multhopp	Aerodynamics of the fuselage. Luft. Vol.18. ARC 5263 (March, 1941).
6	Schlichting	The aerodynamics of the mutual influence between parts of the aircraft. RAE Library Translation No.275 (May, 1949).
7	Haile and Jefferies	Wind tunnel data on the effects of cabins, radiators and similar excrescences on C_{m_0}. ARC 6655. RAE Report No. Aero.1743A (February, 1943). (Unpublished)
8	Young	The aerodynamic characteristics of flaps. ARC 10,766. RAE Report No.2185 (February, 1947). (To be Published)
9	Schlichting	Calculation of the influence of a body on the position of the aerodynamic centre of aircraft with swept-back wings. ARC 10,689. RAE Technical Note No Aero.1879 (March, 1947). (To be Published)

The following papers were used for the comparison of experimental results and estimated values, in Appendix IV.

No.	Author	Title, etc.
10	Mair, Hutton and Gamble	High speed wind tunnel tests on a twin-engined fighter (Hornet). RAE Report No. Aero.1971 (August, 1944).
11	Kirk and Godwin	Wind tunnel tests on a twenty fourth scale model of an eight-engined transport aircraft (Brabazon I). ARC 9618. RAE Report No. Aero.2115 (February, 1946). (Unpublished)

LIST OF REFERENCES (Contd.)

No.	Author	Title, etc.
12	R. Warden	Wind tunnel tests on a 1/12th scale model of a twin-engined Military Transport at N.P.L. (Airspeed C.13/45 Ayrshire) ARC 12,058. (To be Published)
13	-	Type 175, lift, drag and pitching moment tests. Bristol Aeroplane Co. Report F.N.144. (Unpublished)
14	Thompson and Barnes	Wind tunnel tests on the Gloster Whittle F9/40. ARC 4998. RAE Report No. B.A.1648 (December, 1940). (Unpublished)
15	Scholkemeier	Six-component measurements on the G.O.345. A.G.D.1017/G (July, 1944). (Unpublished)
16	Jacobs and Ward	Interference of wing and fuselage from tests of 209 combinations in the N.A.C.A. variable-density wind tunnel. NACA Report No. 540 (1935).

APPENDIX I

Potential flow formulae for ΔC_{m_0} and ΔK_n due to body

1. The formulae of Ref.5 and 6

Using the notation given in this report, it is shown in Ref.5 and 6 that the overall moment on a body in potential flow is

$$M = - \int_L \tfrac{1}{2}\rho V^2 \cdot \frac{\pi}{2} \cdot \frac{d}{dx} (\beta b^2)\, x \cdot dx \quad ,$$

where the origin of reference lies at any point on the body axis, where b = body width.

Integrating by parts and writing in coefficient form

$$C_m = \frac{\pi}{2S\bar{c}} \int_L \beta b^2 \cdot dx \quad ,$$

independent of fore and aft position of origin.

If the body does not affect the wing lift, at $C_L = 0$ the wing has no effect and β = constant, equal to $-i_w$, the angle between body axis and wing no-lift angle.

$$\therefore \; \Delta C_{m_0} \text{ due to body} = - \frac{\pi . i_w}{2S\bar{c}} \int_L b^2 \cdot dx = - \frac{2 i_w \, V_{ol}}{S\bar{c}},$$

i_w being measured in radians.

Again,

$$\frac{dC_m}{d\alpha} = \frac{\pi}{2S\bar{c}} \int_L \frac{d\beta}{d\alpha} \cdot b^2 \cdot dx \, .$$

If the wing lift slope is unaltered by the presence of the body, this gives

$$\Delta K_n \text{ due to body} = - \frac{dC_m}{dC_L} = - \frac{\pi}{2aS\bar{c}} \int_L \frac{d\beta}{d\alpha} \cdot b^2 \cdot dx \, .$$

Wing height and body depth do not appear as variables in either of these formulae, and both ΔC_{m_0} and ΔK_n vary as (body width)^2.

Ahead of the wing $\frac{d\beta}{d\alpha} > 1$ due to upwash, over the wing $\frac{d\beta}{d\alpha} = 0$, and aft of wing $\frac{d\beta}{d\alpha} < 1$ due to downwash. Thus the part of the body ahead of the wing has the dominating effect.

For the models used in the systematic tests, b = the diameter D of the cylindrical body, except for elliptic nose and tapered rear fairings. Writing b^2 on the nose fairing = D^2-(function of nose fairing shape), we have, taking origin at wing L.E.,

$$\Delta K_n \text{ due to body} = -\frac{\pi}{2aS\bar{c}}\left[\int_{-m}^{o}\frac{d\beta}{d\alpha}D^2 \cdot dx - (\text{nose fairing effect}) + \int_{c}^{c+n}\frac{d\beta}{d\alpha}\cdot b^2 \cdot dx \text{ for rear body}\right]$$

$$\propto \frac{-D^2}{aS\bar{c}}\left[m\,\frac{\overline{d\beta}}{d\alpha} - (\text{nose fairing effect}) + (\text{rear body effect})\right]$$

where

$$\frac{\overline{d\beta}}{d\alpha} = \frac{1}{m}\int_{m}^{o}\frac{d\beta}{d\alpha}\cdot dx\ .$$

$$\therefore\ \Delta K_n \text{ due to body} \propto \frac{-cD^2}{aS\bar{c}}\left[\left(\frac{m}{c}\right)\left(\frac{\overline{d\beta}}{d\alpha}\right) - (\text{nose fairing effect}) + (\text{rear body effect})\right]$$

This is the expression quoted in section 6.1 of the report.

2. Evaluation of the formulae for models tested

(i) For 9 in. dia. models on large-span wing, the following values were calculated :-

Body combinations	$-\Delta C_{m_0}$ for $i_w = 2^o$	$-\Delta C_{m_0}$ for $i_w = 6^o$
(1,1)	0.0219	0.0656
(1,2) (2,1)	0.0248	0.0742
(1,3), (2,2), (3,1)	0.0276	0.0828
(1,4) to (4,1)	0.0305	0.0914
(2,4) to (4,2)	0.0334	0.1001
(3,4) (4,3)	0.0363	0.1087
(4,4)	0.0392	0.1175

The values are independent of wing height and fore-and-aft position, and body depth.

For the 13.5 in. dia. bodies, results are multiplied by 2.25.
For the 4.5 in. bodies, results are multiplied by 0.25.
For the small span wing (half area of big wing), values are multiplied by 2.

(ii) In order to evaluate the expression for ΔK_n, charts for $\frac{d\beta}{d\alpha}$ and $\frac{\overline{d\beta}}{d\alpha}$ ahead of the wing are given in Ref.6; the values are based on a plain rectangular wing with no allowance for effects of body on local wing lift distribution.* Behind the wing $\frac{d\beta}{d\alpha} = 1 - \frac{d\varepsilon}{d\alpha}$ and a simple formula for downwash is given in Ref.6. The value of "a", wing lift slope, has been obtained from test measurements. The following values of $-\Delta K_n$ due to body 9 in. dia. on the large span wing were calculated:-

	$-\Delta K_n$ (large span wing, 9 in. dia. body)			
Front body no.	1	2	3	4
Rear body no.1	0.086	0.106	0.125	0.144
2	0.091	0.111	0.130	0.149
3	0.095	0.115	0.134	0.153
4	0.100	0.120	0.139	0.158

The values are independent of wing height and wing-body angle and body depth.

For the 13.5 in. dia. bodies, results are multiplied by 2.25.
For the 4.5 in. dia. bodies, results are multiplied by 0.25.
For the small span wing, $S\bar{c}$ is halved, wing lift slope is altered and $\frac{d\beta}{d\alpha}$ changes according to the charts of Ref.6. The values calculated for large span wing now have to be multiplied by a factor nearly constant for all cases, mean value 2.4.

---

* Allowance for wing shape and body effect on lift seemed an unnecessary refinement, as the simple calculations made here show that the theory only partly agrees with test results in any case.

APPENDIX II

Formula for ΔK_n due to wing root fillets

Consider fillet plan form as rear extension to wing, taken right across body.

The mean quarter chord shift is roughly

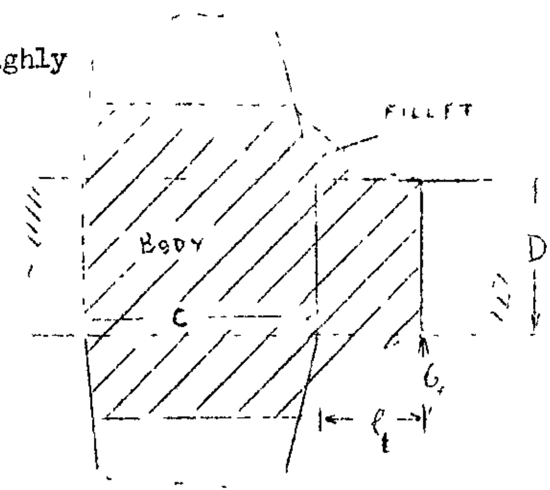

$$\frac{1}{4}\frac{c_f\ S_f}{S\bar{c}}$$

where c_f = mean rearward extension due to fillet

$$= \frac{(\ell_f\ b_f + D\ \ell_f)}{(D + 2\ b_f)} = \frac{(D + b_f)\ell_f}{D + 2\ b_f}$$

while S_f = shaded area = $(D + 2\ b_f)c + (D + b_f)\ell_f$

$$= (D + 2\ b_f)(c + \ell_f) - b_f\ \ell_f$$

$$= (D + 2\ b_f)(c + \ell_f) \text{ approximately.}$$

$\therefore$ centre of pressure shift of wing =

$$\Delta K_n \text{ due to fillet} = \ell_f\ \frac{(C + \ell_f)(D + b_f)}{4\ S\bar{c}}\ .$$

The lengths ℓ_f and b_f are assumed to be those of the fillet outside the maximum width of the body, i.e. the part of the fillet not seen in plan view is ignored.

APPENDIX III

Formula for ΔC_{m_0} due to fillets

Analysing the measured effects at constant α,

$$\Delta C_{m_\alpha}{}' = \Delta C_{m_0}' + \left(\frac{dC_m}{dC_L}\right)\left(\Delta C_L\right) .$$

For the flat plate fillets of "medium" planform

$$\Delta C_L = -0.0055\,\theta \,, \quad \text{(from measured lift change)},$$

and

$$\Delta C_{m_\alpha} = 0.0035\,\theta \quad \text{(from Fig.20)} + 0.01\,\Delta C_L$$

$$= 0.0029\,\theta$$

where θ = fillet lower surface reflex angle.

The corresponding values for a plain flap of the dimensions of the fillets and the body in between (as for Appendix III), have been calculated according to Ref.8, and it is found that

$$\Delta C_{m_\alpha} \text{ (measured)} = 2.07\,\Delta C_{m_\alpha} \text{ (calculated)} \quad \text{and}$$

$$\Delta C_L \text{ (measured)} = 1.3\,\Delta C_L \text{ (calculated)} .$$

For the range of fillet planforms likely full scale, the charts of Ref.8 can be simplified to give ΔC_{m_α} and ΔC_L in terms of fillet dimensions; thus

$$\Delta C_{m_\alpha} \text{ (calc.)} = 0.022\,\lambda_1 \left(\frac{D+b_f}{b}\right)\theta \quad \text{and}$$

$$\Delta C_L \text{ (calc.)} = -0.061\,\lambda_1 \left(\frac{D+b_f}{b}\right)\theta$$

where λ_1 is given in Ref.8.

For the "normal" fillet thickness, the thickness effect was seen in Fig.20 to be about 0.030 on ΔC_{m_0}, nearly independent of θ_f. This can be generalised on the assumption that it varies with fillet overall span and chord; hence

$$(\Delta C_{m_0})\text{thickness} = -0.2\left(\frac{c+\ell_f}{c}\right)\left(\frac{D+b_f}{b}\right)$$

Finally

$$(\Delta C_{m_o}) \text{ due to fillets} = 2.07\,\Delta C_{m_\alpha}\text{ (calc.)} - 1.3\,\frac{dC_m}{dC_L}\,(\Delta C_L)\text{(calc.)}$$

$$+ \text{ thickness effect.}$$

$$= \left[(0.046 + 0.08\,\frac{dC_m}{dC_L})\,\lambda_1\theta - 0.2\left(\frac{c+\ell_f}{c}\right)\right]\left[\frac{D+b_f}{b}\right]$$

where λ_1 is given in Fig.5 of Ref.8 and = 0.5 to 0.6 for normal fillet chords.

If the no-tail C_m is being considered, $\frac{dC_m}{dC_L}$ may be large for an orthodox with-tail aircraft. But if the overall trim change for an orthodox aircraft, or the value of C_{m_o} for a tailless aircraft, is being considered, $\frac{dC_m}{dC_L}$ is usually small enough for the second term in the expression to be ignored.

It will be noted that the formula derived above does not give $\Delta C_{m_o} = 0$ for $\theta = 0$, because the thickness term was unaffected by θ for the range of values of θ used in the analysis. At very different values of θ from those used here we may expect the thickness term to vary in an unknown manner, and for $\theta = 0$, the value of ΔC_{m_o} may or may not equal zero depending on the shape of the wing-body fairing.

When b_f, fillet width, is zero, we should expect $\Delta C_{m_o} = 0$. The above formula, which uses $(D + b_f)$ as a variable, obviously breaks down for very small fillet widths.

APPENDIX IV

Accuracy of generalised methods of prediction, and comparison with other data

1. ΔK_n due to body, no fillets

The following table comparès results from the systematic tests with values estimated by means of the charts of Fig.22:-

Test body	Wing Aspect Ratio	Body dia.	$-\Delta K_n$ due to body	
			Estimated	Measured
(1,3)	5	4.5	0.068	0.068
(3,3)	5	4.5	0.100	0.095
(3,1)	5	9	0.289	0.290
(3,3)	10	4.5	0.042	0.042
(3,3)	10	13.5	0.244	0.258
(2,2)	10	9	0.106	*0.104 to 0.112
(4,2)	10	9	0.148	*0.144 to 0.159

*Range of various wing heights and angles relative to body.

The table shows that the charts reproduce the test results on which they are based to a mean accuracy of $\pm$ 0.004.

The following table compares estimated and measured effects on various aircraft models. All the models were tested without fillets except for the Meteor, Bristol 175 and Stirling. In the first two of these the fillet is very small and cannot have much effect. According to the analysis of Appendix III the fillet should reduce $-\Delta K_n$, but no allowance for it has been made in estimated values given below:-

Aircraft model	Ref. No.	$\frac{m}{c}$	$\frac{n}{c}$	$-\Delta K_n$ due to body	
				Estimated	Measured
Hornet	10	0.26	1.5	0.009	0.011
Brabazon	11	1.98	2.67	0.070	0.076
Ayrshire	12	1.83	2.31	0.107	0.100
Bristol 175	13	1.96	3.32	0.129	≠ 0.105
Meteor	14	0.91	1.6	0.036	0.038
G.0.345	15	1.27	1.65	0.055	0.051
Vampire		0.61	0.18	0.034	0.040
N.A.C.A. model	16	0.12	2.91	0.005	0.002
		0.51	2.52	0.020	*0.009 to 0.015
		0.76	2.27	0.029	*0.022 to 0.030
		1.01	2.02	0.036	*0.038 to 0.044
		1.51	1.52	0.048	0.057

Aircraft Model	Ref. No.	$\frac{m}{c}$	$\frac{n}{c}$	$-\Delta K_n$ due to body	
				Estimated	Measured
Manchester		1.1	2.1	0.029	0.030
Lancaster		1.1	2.1	0.022	0.020
Stirling		1.05	2.1	0.030	0.035
Tapered wing/body		1.34	1.54	0.036	0.038

/ Bristol 175 was tested with 3 angles of wing sweepback. Value quoted here is extrapolation to zero sweepback. Sweepback effects on ΔK_n measured agree quite well with values estimated by Ref.9.

* Extreme values for various wing heights and wing body angles.

The table shows that, apart from the Bristol 175, calculation and measured are within a mean agreement of ± 0.005.

2 ΔK_n due to fillets

The formula in Appendix II, when applied to the systematic test model gives the following comparison with measurement:-

Fillet	$-\Delta K_n$ due to fillets	
	Estimated	Measured
Small	-0.005	*-0.006
Medium	-0.017	*-0.015
Large	-0.044	-0.018

*Mean of all values measured.

The agreement is satisfactory except for the "large" fillet. The large fillet effect depends on a single case, and the zero "no fillet" run was not repeated at the time. It is likely that this single result is wrong. However, the practical size of fillet installations full scale is unlikely to exceed the "medium".

There is very little adequate data from ad hoc tests, but the following table summarises what is available:-

Aircraft Model	Ref. No.	$-\Delta K_n$ due to fillets	
		Estimated	Measured
Brabazon (large)	11	-0.025	-0.005
*Dakota		-0.011	+0.011

* Tested without nacelles, which lie close to wing root.

These results are not in agreement with the formula suggested: it appears that the formula overestimates the stabilising influence. In the case of the Dakota, the test result shows a destabilisation due to fillet, which cannot be conceived in the analysis of Appendix II.

3 ΔC_{m_0} due to body, no fillets.

Comparisons of test measurements with the values shown on the charts of Fig.23 for the systematic test model are given in the following table:-

Test body	Wing Aspect Ratio	Body dia.	i_w deg.	$-\Delta C_{m_0}$ due to body	
				Estimated	Measured
(1,1)	5	4.5	2	0.007	0.009
(3,3)	5	4.5	2	0.0128	0.0135
(3,1)	5	9	2	0.0335	0.030
(3,3)	5	9	2	0.0387	0.033
(1,1)	10	4.5	2	0.0035	0.0035
(3,3)	10	4.5	2	0.0064	0.0055
(1,4)	10	9	2	0.0135	*0.0185 to 0.0125
(2,2)	10	9	2	0.0154	*0.014 to 0.0175
(2,2)	10	9	6	0.0461	*0.0465, 0.0545
(1,4)	10	9	6	0.0403	0.047
(3,3)	10	13.5	2	0.0402	0.042

* Means for various wing heights.

The table shows that, apart from (1,1) 4.5 in. dia., and the high value for (1,4) 10 in. dia., the values estimated are all within 20% of the original test results. Of the two exceptions, the first is numerically too small to expect a high accuracy, and the second refers to low wing, no fillets, which is a case which does not occur full scale.

The following table compares test results on aircraft models without fillets, the exception being the Bristol 175 which had a small fillet of unknown dimensions:-

Aircraft model	Ref. No.	$\frac{L}{D}$	i_w deg.	$-\Delta C_{m_0}$ due to body		Remarks
				Estimated	Measured	
Hornet	10	10	3.7	0.0047	0.004	
Brabazon	11	9.45	5.9	0.031	0.053, 0.047	Without and with wires on wing surface.
Ayrshire	12	7.3	2.6	0.017	0.045	Turned-up rear. Square body.
Bristol 175	13	9.8	4.7	0.0345	0.047	Turned-down nose. Small fillet.
G.0.345	15	7.4	-5.5	0.020	0.033	Inaccurate data.
Vampire		4.45	0.5	0.001	0.008	Turned-down nose and large cabin.

Aircraft Model	Ref. No.	$\frac{L}{D}$	i_w deg.	$-\Delta C_{m_0}$ due to body		Remarks
				Estimated	Measured	
N.A.C.A. Model	16	5.86	8	0.016 0.019 0.016	0.025 0.029 0.018	Mid.wing. Two fore-and-aft positions. High or low wing.
Manchester		11	6.5	0.0125	0.0125	
Lancaster		11	6.5	0.010	0.007	
Tapered wing/body		11.8	4.5	0.0135	0.026	

Difficulty arises in defining the body axis in some cases. The mid-height line was taken for the Hornet; no allowance was made for the turned-down nose shapes.

It is seen that the calculation agrees with measurement in 4 out of the 12 cases listed. In the other 8 cases, the calculation underestimates, on an average, by one third to a half.

4 ΔC_{m_0} due to fillets

The formula of Appendix III, when applied to the systematic test model, gives the following comparison for the fillets of "normal" thickness:-

Fillet size	θ deg.	$-\Delta C_{m_0}$ due to fillets		Remarks
		Estimated	Measured	
Small	12	-0.006	-0.006	Mean for $i_w = 2^o$.
Medium	8	+0.001	-0.004	)Mean for (1,2) and (1,4) at
(nose(1))	12	-0.013	-0.015	)$i_w = 2^o$ and 6^o.
	16	-0.028	-0.024	)
Medium (nose 4)	12	-0.017	-0.018	Mean for all noses (4) at $i_w = 2^o$.
Large	12	-0.024	-0.015	Single reading (2,2).

The variation with θ, the reflex angle, is slightly overestimated because of the simplification in the analysis that the thickness effect was independent of θ (the "normal" thickness line and the flat plate line in Fig.20 are not quite parallel). The large-fillet effect is overestimated; this is the same as for ΔK_n due to fillets. The greater value of $\frac{dC_m}{dC_L}$ for front body (4) compared with front body (1) is reflected in measurement and estimate by an increase in ΔC_{m_0} due to fillets.

Comparison with available ad hoc data gives the following table:-

Aircraft Model	Ref. No.	$-\Delta C_{m_0}$ due to fillets	
		Estimated	Measured
Brabazon	11	-0.030	-0.012
*Dakota		+0.007	+0.002

*Tested without nacelles (which lie close to wing root).

The overestimation on the Brabazon might possibly be connected with a shielding effect of the wing (21% thick, 3.3% camber, cusped section) at the low test Reynolds number. The changed sign for the Dakota fillet (due to the small amount of reflex) is reproduced in the estimate.

TABLE I

MODEL DETAILS

WING		Large Span	Small span
Gross area (tapered to centre line)	– S	980.1 sq.in.	490 sq.in.
Span	– b	99 in.	49.5 in.
Mean chord	– $\bar{c}$	9.9 in.	9.9 in.
Centre line chord	– c_o	13.5 in.	13.5 in.
Root chord.	– c	12.54 in.	– (for 13.5 in. dia. body)
		12.86 in.	– (for 13.5 × 9 in. body)
		12.86 in.	12.22 in. (for 9 in. dia. body)
		13.18 in.	12.86 (for 4.5 in. dia. body)
Aspect Ratio		10	5
Taper Ratio		2 : 1	2 : 1
Centre line t/c		18%	18%
Centre line section		N.A.C.A.2418	N.A.C.A.2418
Tip t/c		12%	12%
Tip section		N.A.C.A.2412	N.A.C.A.2412
Camber		2%	2%
Dihedral		Upper surface horizontal	Upper surface horizontal
Sweepback of $\frac{1}{4}$ chord line		0^o	0^o
Twist		0^o	0^o

BODY For all bodies:-

Elliptic normal nose fairing length 16.2 in. = 1.2 c_o
Elliptic short nose fairing length 7.2 in = 0.53 c_o
Tapered symmetrical rear fairing length 27 in. = 2 c_o
Tapered turned-up rear fairing length 27 in. = 2 c_o
Body diameters D 4.5 in. 9 in. 13.5 in. also 13.5 in. deep × 9 in. wide.

Body lengths:-
m, m_o = body front length measured from L.E. of root and centre line chords respectively: n, n_o = body rear lengths measured from T.E. of root and centre-line chords respectively.

Body	Front length - inches						
	m_o	$\frac{m_o}{c_o}$	m: A = 10			A = 5	
			13.5 in.	9 in.	4.5 in.	9 in.	4.5 in.
1	20.2	1.5	20.44	20.36	20.28	20.52	20.36
2	26.5	1.96	26.74	26.66	26.58	26.82	26.66
3	32.8	2.43	33.04	32.96	32.88	33.12	32.96
4	39.1	2.9	39.34	39.26	39.18	39.42	39.26

	Rear length - inches						
	n_o	$\frac{n_o}{c_o}$	n				
			A = 10			A = 5	
1	28.3	2.1	29.02	28.78	28.54	29.26	28.78
2	34.6	2.57	35.32	35.08	34.84	35.56	35.08
3	40.9	3.03	41.62	41.38	41.14	41.86	41.38
4	47.2	3.5	47.92	47.68	47.44	48.16	47.68

Total body length, L, is obtained by adding front, m_o, and rear-body length, n_o, and c_o = 13.5 in. Values of N used in Fig.24 are obtained by adding $\frac{3c_o}{4}$ = 10.1 in. to values of n_o. For N/D, divide by appropriate body diameter.

WING-BODY JUNCTION

Height of wing centre line quarter chord point:-

Low wing 3.10 in. below body centre-line
Mid wing on body centre-line
High wing 2.60 in. above body centre-line

Wing-body angle:-

Geometric 0° and 4°

Aerodynamic, i_W 2° and 6° (measured relative to wing no-lift line).

Wing was pivoted about wing centre-line quarter chord point.

C.G.POSITION

Pitching moments measured in test about wing centre-line quarter chord point;
Pitching moment results referred to wing mean quarter chord point.

TABLE II

Comparison of aircraft dimensions with test model

Some dimensions are approximate. Test model refers to 9 in. dia. bodies on large-span wing.

$\bar{c}$ = mean chord; c = root chord, D = body dia. at wing L.E.;

m = body front length ahead of L.E. root chord;

n = body rear length aft of T.E. root chord;

		Tudor I	Tudor II	Hermes	Apollo	Brabazon	Bristol 175	Test model
Wing	Camber %	1.6	1.6	1.5	2.5	3.3	2 (root)	2
	Dihedral	3.5°	3.5°	3.5°	4.5°	3°	5°	1°
	Root t/c %	18	18	21	18	21	17	18
	Tip t/c %	8	8	7	18	15	13	12
	Aspect Ratio	10	10	9.1	8.7	9.9	9.5	10
	Taper Ratio	3	3	2.6	2	3	3.3	2
	$\bar{c}/c$	0.75	0.75	0.78	0.78	0.76	0.65	0.77
	Wing/body angle	4°	4°	2°	0°	3.5°	3°	0° and 4°
Body	D/c	0.63	0.69	0.69	0.78	0.60	0.62	0.70
	m/c	1.4	2.0	1.6	1.9	2.0	1.9	1.58 to 3.05
	n/c	2.6	3.0	2.5	2.5	2.6	2.9	2.24 to 3.71

TABLE III

Aerodynamic characteristics of large and small span wings

Wing Aspect Ratio	α°	C_L	C_D	C_m
10	-3.9	-0.149	0.0124	-0.0562
	-2.3	-0.029		-0.0518
	-0.75	0.105		-0.0473
	0.8	0.231	0.0122	-0.0430
	2.4	0.351		-0.0381
	3.9	0.475		-0.0347
	5.5	0.609	0.0237	-0.0346
	7.05	0.739		-0.0352
	8.6	0.866		-0.0330
	10.15	0.945	0.0473	-0.0225
	11.7	1.013		-0.0122
	13.2	1.086		-0.0037
	14.7	1.131	0.0755	+0.0015
	16.3	1.149		-0.0008
	17.75	1.149		-0.0099
	19.15	0.922		
5	-3.6	-0.080		-0.0550
	-2.6	-0.018	0.0126	-0.0511
	-1.6	0.040	0.0120	-0.0469
	-0.55	0.100	0.0124	-0.0434
	0.95	0.196	0.0132	-0.0380
	2.45	0.286		-0.0315
	4.0	0.380	0.0196	-0.0257
	5.5	0.481		-0.0209
	7.05	0.586	0.0335	-0.0192
	8.55	0.689		-0.0184
	10.1	0.776	0.0540	-0.0133
	11.6	0.849		-0.0047
	13.6	0.937		
	15.65	1.013		
	18.65	1.098		
	21.6	0.825		

TABLE IV

Typical lift and pitching moment measurements on body combinations

Range of front body lengths on rear body (4). Low wing, 9 in. dia. body, Medium fillets, large span wing, $i_W = 6^\circ$.

Pitching moments referred to wing mean quarter chord point.

α deg.	C_L	C_M	ΔC_M due to body	C_L	C_M	ΔC_M due to body
		Body (1,4)			Body (2,4)	
-2.55	-0.105	-0.0922	-0.0365	-0.104	-0.1031	-0.0473
-1.5	-	-	-	-0.021	-0.0899	-0.0374
-1.0	0.021	-0.0778	-0.0268	+0.021	-0.0844	-0.0334
-0.25	-	-	-	0.084	-0.0756	-0.0270
0.6	0.155	-0.0634	-0.0174	0.158	-0.0656	-0.0198
1.35	-	-	-	0.213	-0.0576	-0.0143
2.1	0.282	-0.0495	-0.0081	0.281	-0.0483	-0.0068
3.7	0.419	-0.0342	0.0034	0.421	-0.0317	0.0056
5.25	0.551	-0.0211	0.0137	0.556	-0.0159	0.0188
6.85	0.696	-0.0106	0.0234	0.702	-0.0021	0.0320
8.4	0.820	-0.0013	0.0327	0.824	+0.0107	0.0444
		Body (3,4)			Body (4,4)	
-2.55	-0.111	-0.1111	-0.0552	-	-	-
-1.5	-0.021	-0.0978	-0.0453	-0.003	-0.1043	-0.0525
-1.0	0.027	-0.0906	-0.0398	0.035	-0.0979	-0.0475
-0.25	0.085	-0.0800	-0.0314	0.101	-0.0853	-0.0374
0.6	0.152	-0.0686	-0.0226	0.174	-0.0731	-0.0281
1.35	0.209	-0.0601	-0.0162	0.228	-0.0627	-0.0195
2.1	0.278	-0.0485	-0.0070	0.298	-0.0508	-0.0098
3.7	0.418	-0.0276	0.0099	0.436	-0.0263	0.0107
5.25	0.549	-0.0096	0.0251	0.567	-0.0058	0.0288
6.85	0.689	0.0043	0.0383	0.726	0.0115	0.0459
8.4	0.829	0.0210	0.0546	0.846	0.0297	0.0627

TABLE V

Change in aerodynamic centre and C_{m_0} due to body, no fillets

9" diameter body, large span wing

The low wing measurements marked * were made separately from the other tests.

Wing height	Body	$-\Delta K_n$ $i_w = 2^\circ$		$-\Delta K_n$ $i_w = 6^\circ$	$-\Delta C_{m_0}$ $i_w = 2^\circ$		$-\Delta C_{m_0}$ $i_w = 6^\circ$
Low	1,1	0.078		0.082	0.013		0.045
	1,2	0.081		0.083	0.0165		0.0485
	1,3		0.097*			0.017*	
	1,4	0.092			0.0185		
	2,2	0.107		0.104	0.0175		0.0545
	2,3	0.106	0.121*		0.0195	0.0195*	
	2,4	0.114			0.022		
	3,3		0.146*			0.022*	
	3,4		0.140*			0.0225*	
	4,3		0.163*			0.0235*	
	4,4		0.158*			0.0230*	
Mid		Set A	Set B		Set A	Set B	
	1,1	0.084	0.080	0.073	0.011	0.010	0.035
	1,2	0.088	0.083	0.077	0.0135	0.0105	0.0395
	1,3		0.0885	0.088		0.012	0.043
	1,4	0.098	0.094	0.087	0.015	0.0135	0.047
	2,1	0.110		0.101	0.0145		0.044
	2,2	0.112	0.106	0.105	0.017	0.014	0.0465
	2,3	0.115	0.1085	0.110	0.019	0.015	0.048
	2,4	0.113		0.110	0.016		0.055
	3,1	0.128		0.116	0.0165		0.0515
	3,2	0.136	0.127	0.123	0.021	0.016	0.0535
	3,3		0.129	0.1245		0.017	0.057
	3,4			0.128			0.0615
	4,1	0.145		0.141	0.018		0.0585
	4,2	0.159	0.152	0.144	0.0235	0.019	0.061
	4,3		0.152	0.144		0.0195	0.0645
	4,4			0.150			0.0700
High	1,1	0.076			0.0095		
	1,2	0.082			0.011		
	1,3	0.088			0.0115		
	1,4	0.090			0.0125		
	2,1	0.104			0.014		
	2,2	0.106			0.0145		
	2,3	0.111			0.016		
	2,4	0.115			0.0165		
	3,1	0.129			0.0175		
	3,2	0.129			0.0175		
	3,3	0.135			0.019		
	3,4	0.137			0.019		
	4,1	0.149			0.0205		
	4,2	0.150			0.020		
	4,3	0.152			0.021		
	4,4	0.155			0.0195		

TABLE VI

Effect of Turned-Up Rear End of Body

9" diameter body, large span wing

Datum cases marked with * were repeated at same time as turned-up body tests.

Wing Position	i_W	Body	$-\Delta K_n$		$-\Delta C_{m_0}$	
			Symmetrical Rear	Turned-Up Rear	Symmetrical Rear	Turned-Up Rear
Low (with medium fillets)	2°	2,2	0.095*	0.092	0.0035*	0.0020
		2,3	0.098*	0.094	0.0045*	-0.001
		2,4	0.104*	0.099	0.0035*	-0.002
	6°	2,2	0.092	0.084	0.0315	0.027
		2,3	0.097*	0.090	0.0335*	0.027
		2,4	0.102	0.096	0.0355	0.027
High	2°	2,2	0.108*	0.099	0.013*	0.009

TABLE VII

Effect of Nose Shape Variation and Cabin

9" diameter body, large span wing, $i_W = 6°$
low wing, medium fillets
Total body front length is not altered by change in nose-shape

Normal fairing case was tested at same time as
both shorter nose and cabin tests

Body	Nose Shape	$-\Delta K_n$	$-\Delta C_{m_0}$
1,1	Normal elliptic fairing	0.071	0.0227
1,1	Shorter " "	0.080	0.0254
3,1	Normal " "	0.117	0.0370
3,1	Shorter " "	0.124	0.0392
3,4	Normal " "	0.125	0.043
3,4	Cabin nose-piece	0.123	0.0455

TABLE VIII

Effect of varying body diameter and depth and wing span

Mid Wing $i_w = 2^o$

The "ratio" tabulated is the value for 4.5" or 13.5" diameter bodies divided by the value for the 9" body.

Body Combination	Body size	$-\Delta K_n$				$-\Delta C_{m_o}$			
		A = 10 wing		A = 5 wing		A = 10 wing		A = 5 wing	
		Values	Ratio	Values	Ratio	Values	Ratio	Values	Ratio
1,1	4.5" Dia.	0.026	0.32	0.064	0.35	0.0035	0.35	0.0090	0.46
	9" Dia.	0.082	1	0.184	1	0.0100	1	0.0195	1
	13.5" Dia.	0.146	1.8			0.0225	2.3		
	9" × 13.5"	0.084	-			0.011	-		
1,3	4.5" Dia.	0.028	0.32	0.068	0.34	0.0035	0.30	0.0095	0.38
	9" Dia.	0.088	1	0.199	1	0.0115	1	0.0250	1
	13.5" Dia.	0.165	1.9			0.030	2.6		
	9" × 13.5"	0.096	-			0.0145	-		
3,1	4.5" Dia.	0.040	0.32	0.092	0.32	0.0055	0.38	0.0115	0.38
	9" Dia.	0.125	1	0.290	1	0.0145	1	0.0300	1
	13.5" Dia.	0.241	1.9			0.034	2.3		
	9" × 13.5"	0.135	-			0.0145	-		
3,3	4.5" Dia.	0.042	0.31	0.095	0.31	0.0055	0.31	0.0135	0.41
	9" Dia.	0.137	1	0.321	1	0.0175	1	0.0330	1
	13.5" Dia.	0.258	1.9			0.042	2.4		
	9" × 13.5"	0.149	-			0.019	-		

TABLE IX

Change in aerodynamic centre and C_{m_0} due to body, medium fillets

9" dia. body. Large span wing. Low wing.
Normal fillet shape. Reflex θ = 12° and 16°

Body	$-\Delta K_n$		$-\Delta C_{m_0}$	
	$i_w = 2°$	$i_w = 6°$	$i_w = 2°$	$i_w = 6°$
1,1	0.067	0.067	0.002	0.022
1,2	0.068	0.070	0.001	0.025
1,3	0.079	0.074	0.0005	0.0275
1,4	0.079	0.075	0.0015	0.0285
2,1	0.090	0.089	0.0035	0.030
2,2	0.093	0.092	0.004	0.0315
2,3	0.095	0.098	0.0035	0.0335
2,4	0.102	0.102	0.0035	0.0355
3,1	0.107	0.115	0.004	0.038
3,2	0.112	0.117	0.0055	0.039
3,3	0.120	0.123	0.005	0.042
3,4	0.120	0.125	0.0055	0.043
4,1	0.126	0.136	0.008	0.0435
4,2	0.132	0.138	0.008	0.0455
4,3	0.130	0.143	0.0035	0.049
4,4	0.137	0.144	0.006	0.052

TABLE X

Change in aerodynamic centre and C_{m_0} due to body, small and large fillets

9" dia. body. Large span wing. Low wing.
Normal fillet shape. Reflex θ = 12° and 16°

Fillet Size	Body	$-\Delta K_n$		$-\Delta C_{m_0}$	
		$i_w = 2°$	$i_w = 6°$	$i_w = 2°$	$i_w = 6°$
Small	1,1		0.072		0.035
Small	1,4	0.092		0.120	
Small	2,2	0.100	0.101	0.011	0.045
Small	2,3	0.108		0.0130	
Small	2,4	0.116		0.0147	
Small	3,2	0.121		0.0132	
Small	4,1	0.146		0.0140	
Large	2,2	0.090		0.0025	

TABLE XI

Effect of fillet reflex and thickness on $-\Delta K_n$ and $-\Delta C_{m_0}$ due to body

9" dia. body. Large span wing. Low wing.
The no-fillet and with-fillet measurements were made at the same time.

Body	i_w	Reflex Angle θ	Fillet Thickness	$-\Delta K_n$	$-\Delta C_{m_0}$
1,2	2°	no fillet	-	0.081	0.0165
		8°	normal	0.070	0.0135
		12°	"	0.071	0.0035
		16°	"	0.069	-0.0060
1,4	2°	no fillet	-	0.092	0.0185
		8°	normal	0.0775	0.0133
		12°	"	0.079	0.0040
		16°	"	0.080	-0.0067
		12°	Fillet filled out	0.073	0.0096
1,2	6°	no fillet	-	0.083	0.0483
		12°	normal	0.069	0.0320
		16°	normal	0.070	0.0233
		16°	flat plate	0.050	-0.0096
		20°	flat plate	0.043	-0.0230

TABLE XII

Effect of fillets compared with no-fillet measurements

$9''$ dia. body. Large span wing. Low wing.

For ΔK_n the no-fillet datum values are means for all wing heights and values (because insufficient and scattered values measured for low wing).

For ΔC_m the no-fillet datum values are those actually measured for low wing.

In all tests a fillet was fitted in both port and starboard wing-body junctions.

Body	Fillet Size	Fillet Thickness	Fillet reflex θ deg.		Change in $-\Delta K_n$ due to fillets		Change in $-\Delta C_{L_0}$ due to fillets	
			$i_W = 2^\circ$	$i_W = 6^\circ$	$i_W = 2^\circ$	$i_W = 6^\circ$	$i_W = 2^\circ$	$i_W = 6^\circ$
From Tables IX and X								
1,1	Small	Normal	-	16	-	-0.006	-	-0.010
1,4			12	-	0	-	-0.0045	-
2,2			12	16	-0.008	-0.007	-0.0065	-0.0095
2,3			12	-	-0.0025	-	-0.0065	-
2,4			12	-	+0.003	-	-0.0073	-
3,2			12	-	-0.008	-	-	-
4,1			12	-	+0.001	-	-	-
1,1	Medium	Normal	12	16	-0.011	-0.011	-0.011	-0.023
1,2			12	16	-0.014	-0.012	-0.0155	-0.0235
1,3			12	16	-0.012	-0.017	-0.0165	-
1,4			12	16	-0.013	-0.017	-0.017	-
2,1			12	16	-0.015	-0.016	-	-
2,2			12	16	-0.015	-0.016	-0.0135	-0.023
2,3			12	16	-0.0155	-0.0125	-0.016	-
2,4			12	16	-0.011	-0.011	-0.0185	-
3,1			12	16	-0.017	-0.009	-	-
3,2			12	16	-0.017	-0.012	-	-
3,3			12	16	-0.015	-0.012	-0.017	-
3,4			12	16	-0.015	-0.010	-0.017	-
4,1			12	16	-0.019	-0.009	-	-
4,2			12	16	-0.019	-0.013	-	-
4,3			12	16	-0.023	-0.010	-0.020	-
4,4			12	16	-0.017	-0.010	-0.017	-
2,2	Large	Normal	12	-	-0.018	-	-0.015	-
From Table XI.								
1,2	Medium	Normal	8	12	-0.011	-0.013	-0.003	-0.0165
1,4			8	-	-0.0145	-	-0.0052	-
1,2		Normal	12	16	-0.011	-0.014	-0.013	-0.025
1,4			12	-	-0.013	-	-0.0145	-
1,2		Normal	16	-	-0.013	-	-0.0225	-
1,4			16	-	-0.012	-	-0.0252	-
1,4		Filled out	12	-	-0.019	-	-0.0089	-
1,2		Flat plate	-	16	-	-0.032	-	-0.0575
1,2		Flat plate	-	20	-	-0.039	-	-0.0715

TABLE XIII

Analysis of test results on ΔK_n due to body (see section 6.1 of text)

$$\text{No fillets } \Delta = (-\Delta K_n) \cdot \frac{aS\bar{c}}{cD^2}$$

Wing Aspect Ratio	Body Combination	$\frac{m}{c}$	$\frac{n}{c}$	Δ_{10} or Δ_5'			$k = \frac{\Delta(\text{dia. } D)}{\Delta(\text{dia. } 9 \text{ in.})}$	
				13.5 in. dia.	9 in. dia.	4.5 in. dia.	13.5 in. dia.	4.5 in. dia.
10	1,1	1.58	2.24	2.80	3.43	4.56	0.82	1.33
	1,2		2.73		3.57			
	1,3		3.22	3.16	3.88	4.74	0.81	1.22
	1,4		3.71		4.02			
	2,1	2.06	2.24		4.56			
	2,2		2.73		4.67			
	2,3		3.22		4.79			
	2,4		3.71		4.93			
	3,1	2.56	2.24	4.64	5.42	6.96	0.85	1.29
	3,2		2.73		5.62			
	3,3		3.22	5.00	5.65	7.26	0.88	1.29
	3,4		3.71		5.73			
	4,1	3.05	2.24		6.39			
	4,2		2.73		6.58			
	4,3		3.22		6.55			
	4,4		3.71		6.64			
5	1,1	1.58	2.24		2.96	4.16		1.41
	1,3		3.22		3.18	4.38		1.36
	3,1	2.56	2.24		4.75	6.02		1.27
	3,3		3.22		5.08	6.23		1.23

Body	Ratio Δ_5/Δ_{10}		Mean Value
	9 in. dia.	4.5 in. dia.	
1,1	0.86	0.91	0.87
1,3	0.82	0.91	
3,1	0.88	0.86	
3,3	0.90	0.86	

Δ_5 = value of Δ for A.R. = 5 wing.

Δ_{10} = value of Δ for A.R. = 10 wing.

TABLE XIV

Analysis of test results on ΔC_{m_0} due to body without fillets

Bodies of revolution only. $f = (-\Delta C_{m_0}) \cdot \dfrac{S\bar{c}}{\mathrm{Vol.}\, i_W}$

Body	$\frac{L}{D}$	Wing A	Body dia. D in.	Mean $(-\Delta C_{m_0})$ $i_W = 2^\circ$ all wing heights	* $(-\Delta C_{m_0})$ $i_W = 6^\circ$ Mid wing only	Value of f $i_W = 2^\circ$	Value of f $i_W = 6^\circ$
1,1	6.9	10	9	0.011	0.035	0.0175	0.019
1,2	7.6			0.013	0.0395	0.0185	0.0185
1,3	8.3			0.0135	0.043	0.017	0.018
1,4	9.0			0.015	0.047	0.017	0.018
2,1	7.6			0.0145	0.044	0.0205	0.021
2,2	8.3			0.016	0.0465	0.0205	0.0195
2,3	9.0			0.0175	0.048	0.020	0.0185
2,4	9.7			0.018	0.055	0.019	0.019
3,1	8.3			0.017	0.0515	0.0215	0.022
3,2	9.0			0.018	0.0535	0.021	0.0205
3.3	9.7			0.019	0.057	0.020	0.020
3,4	10.4			0.0205	0.0615	0.020	0.020
4,1	9.0			0.019	0.0585	0.022	0.0225
4,2	9.7			0.021	0.061	0.022	0.0215
4,3	10.4			0.0215	0.0645	0.021	0.0205
4,4	11.1			0.021	0.070	0.019	0.021
1,1	4.6	10	$13\frac{1}{2}$	0.0225		0.016	
1,3	5.5			0.030	*The three	0.017	
3,1	5.5			0.034	values for	0.019	
3,3	6.5			0.042	low wing	0.0195	
1,1	13.8	10	$4\frac{1}{2}$	0.0035	omitted	0.0225	
1,3	16.6			0.0035	as all	0.018	
3,1	16.6			0.0055	about	0.028	
3,3	19.4			0.0055	0.008	0.023	
1,1	6.9	5	9	0.0195	higher and	0.155	
1,3	8.3			0.025	would not	0.016	
3,1	8.3			0.030	give fair	0.019	
3,3	9.7			0.033	mean value	0.0175	
1,1	13.8	5	$4\frac{1}{2}$	0.009		0.028	
1,3	16.6			0.0095		0.024	
3,1	16.6			0.0115		0.029	
3,3	19.4			0.0135		0.0285	

Wt.2098 CP18 K3 Printed in Great Britain

FIG. 1.

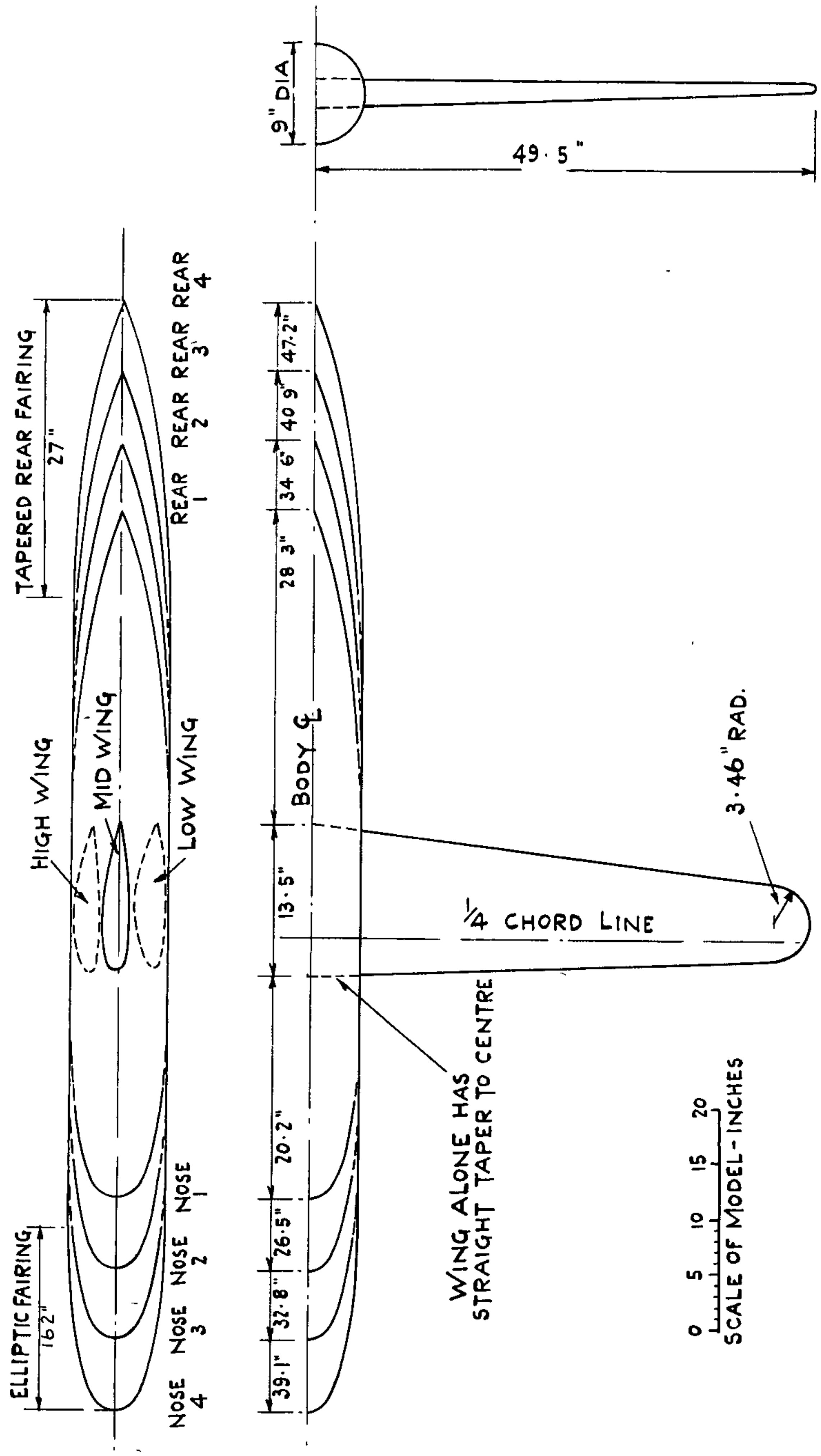

FIG. 1. G.A. OF LARGE SPAN WING AND 9" DIA. BODIES.

FIG. 2. G.A. OF 4.5" DIA: 9X13.5" & 13.5" DIA. BODIES.

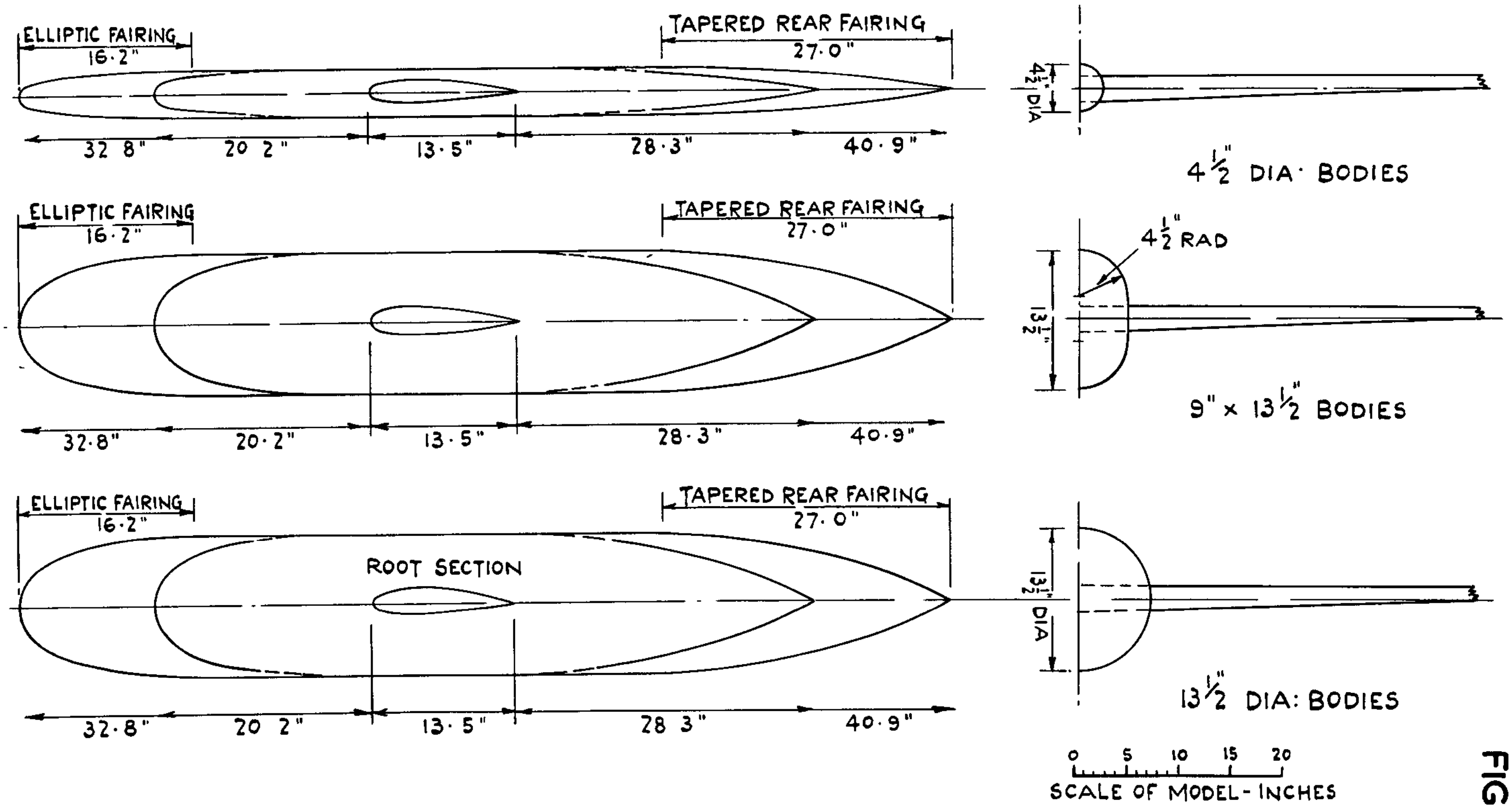

FIG. 2.

FIG. 3. MISCELLANEOUS MODEL DETAILS.

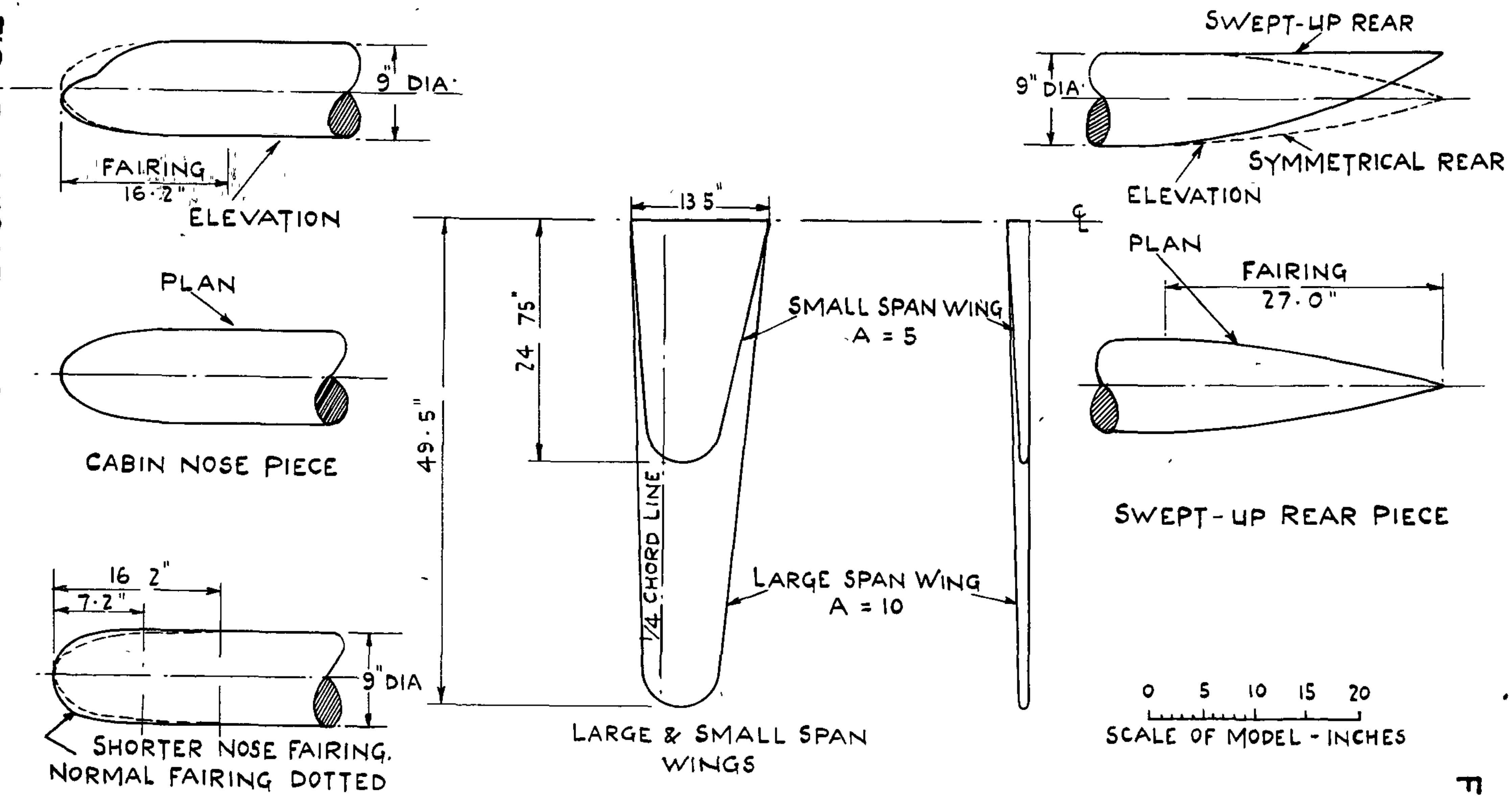

FIG. 3.

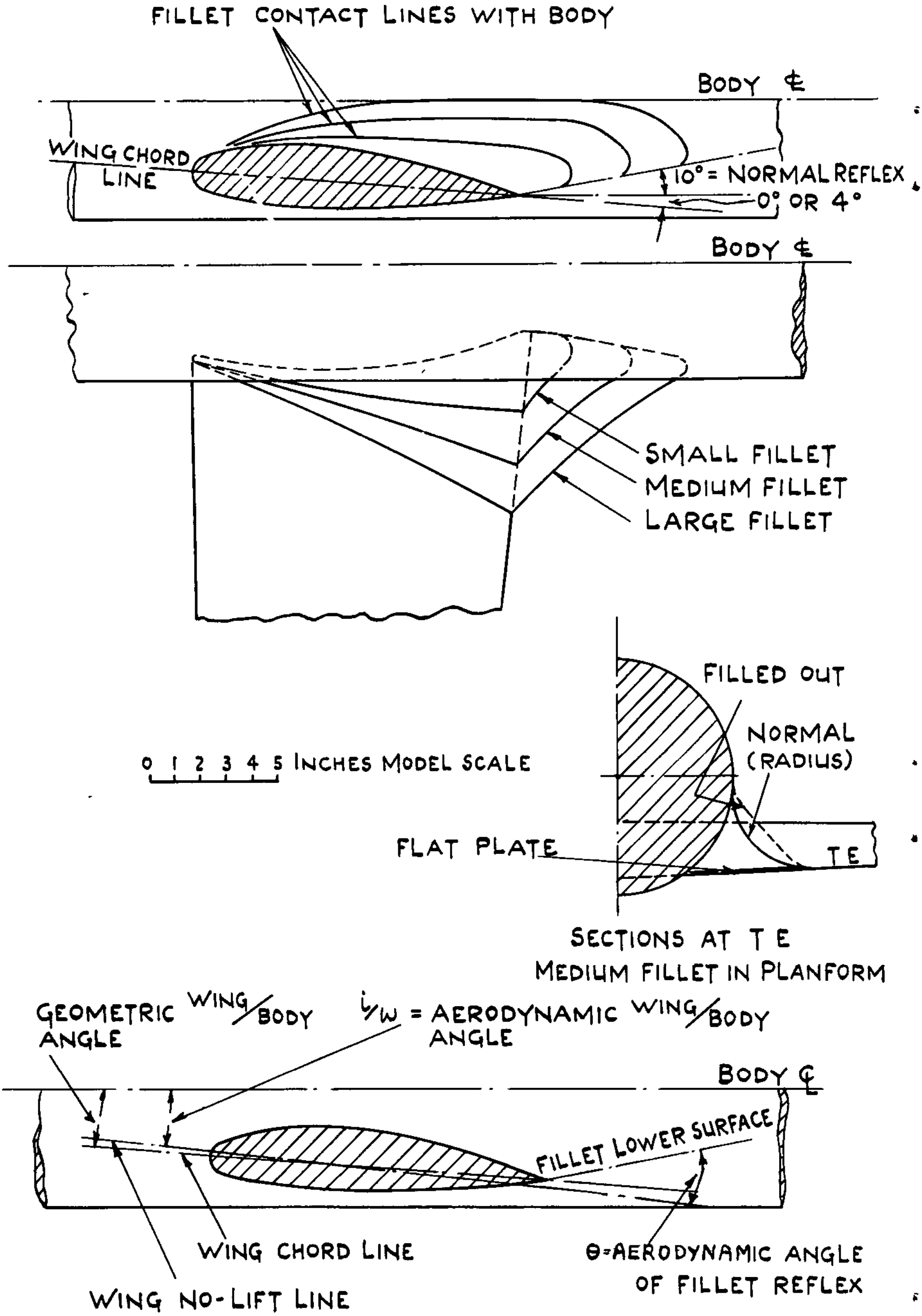

FIG. 4. DETAILS OF FILLETS.

LOW WING, 9" DIA: BODY, LARGE SPAN WING

FIG. 5.

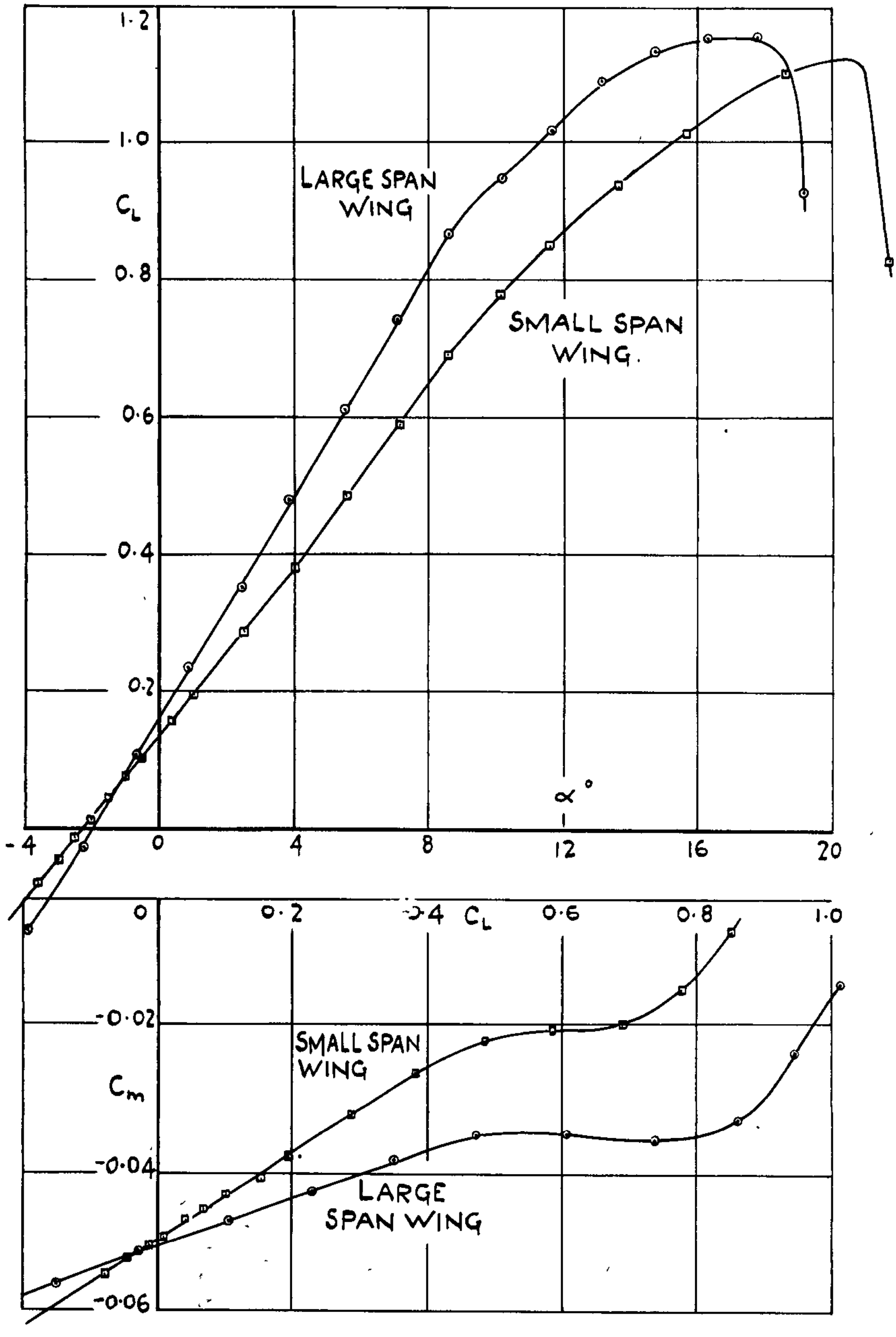

FIG.5. CHARACTERISTICS OF WING ALONE.

FIG. 6.

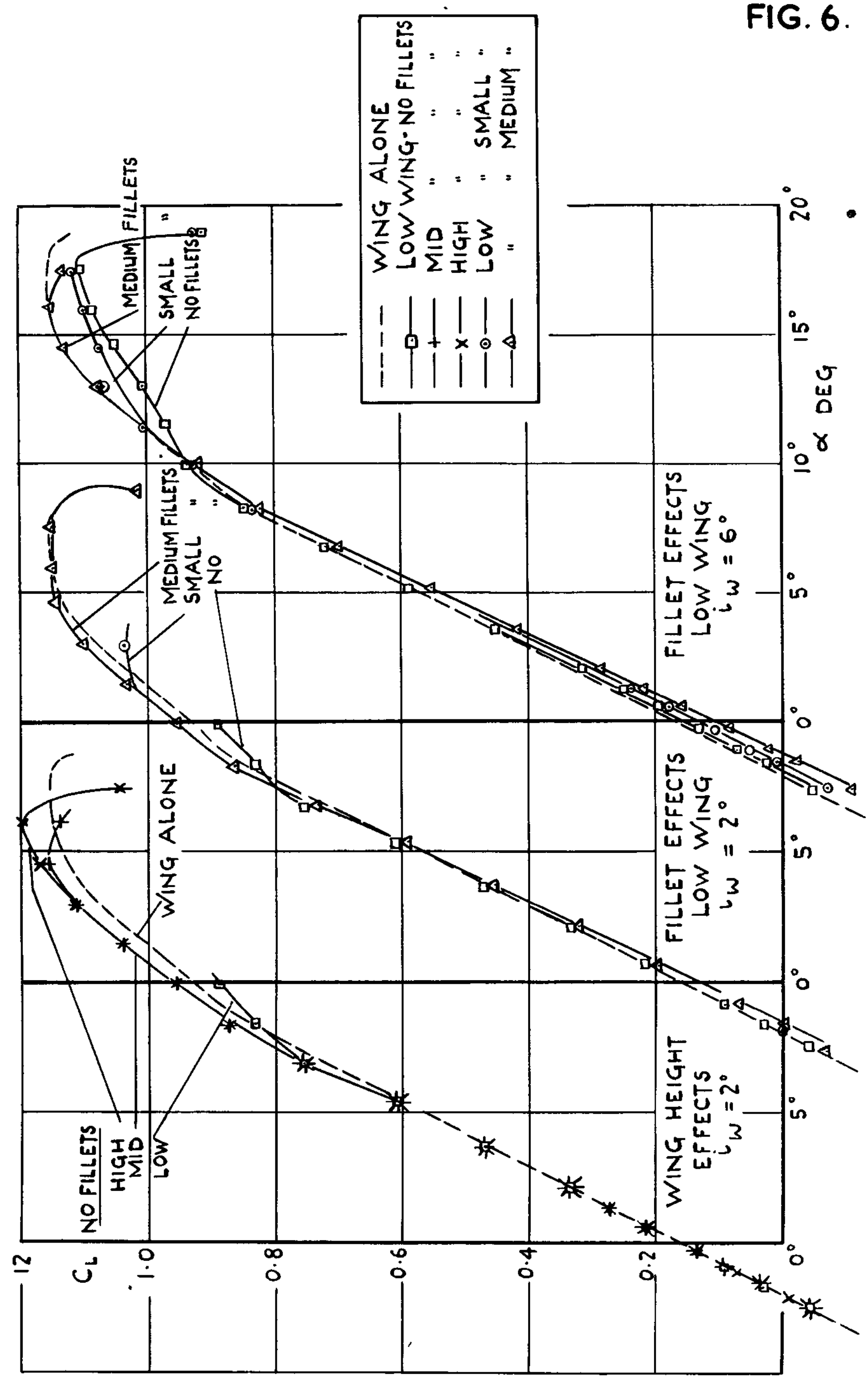

FIG. 6. EFFECT OF WING HEIGHT AND ANGLE AND WING ROOT FILLETS ON LIFT.

NORMAL FILLET SHAPE AND REFLEX, BODY (2,2), 9" DIA: LARGE SPAN WING.

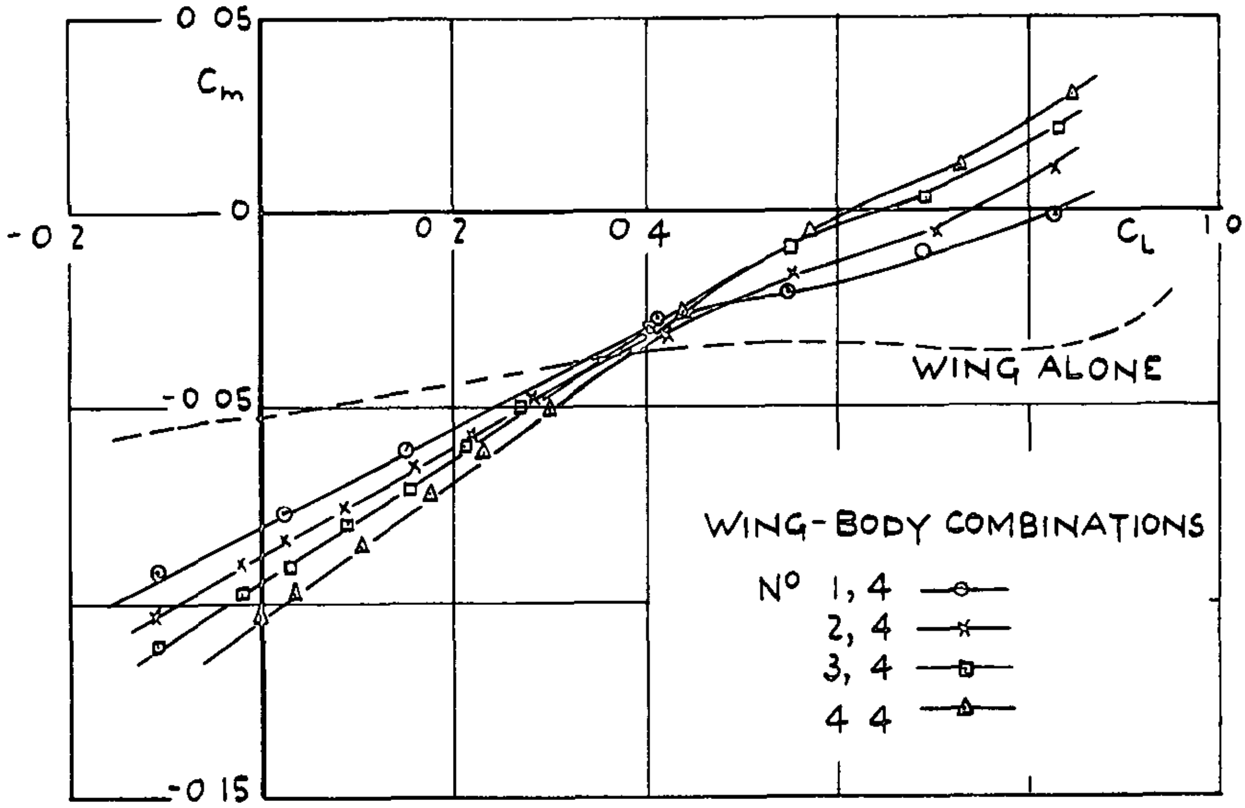

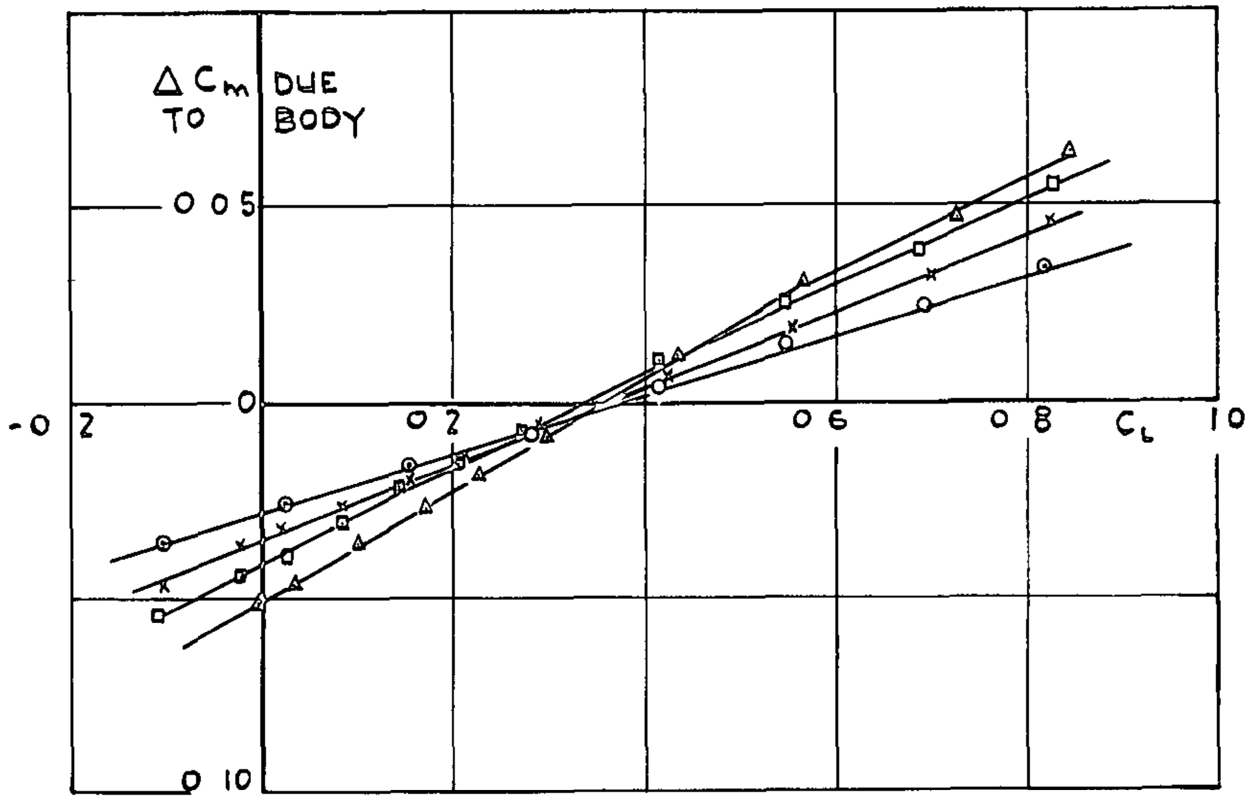

FIG 7 PITCHING MOMENTS FOR RANGE OF FRONT BODY LENGTHS ON REAR BODY N°(4)

LOW WING, 9 DIA BODY, MEDIUM FILLETS, LARGE SPAN WING, $\iota_W = 6°$

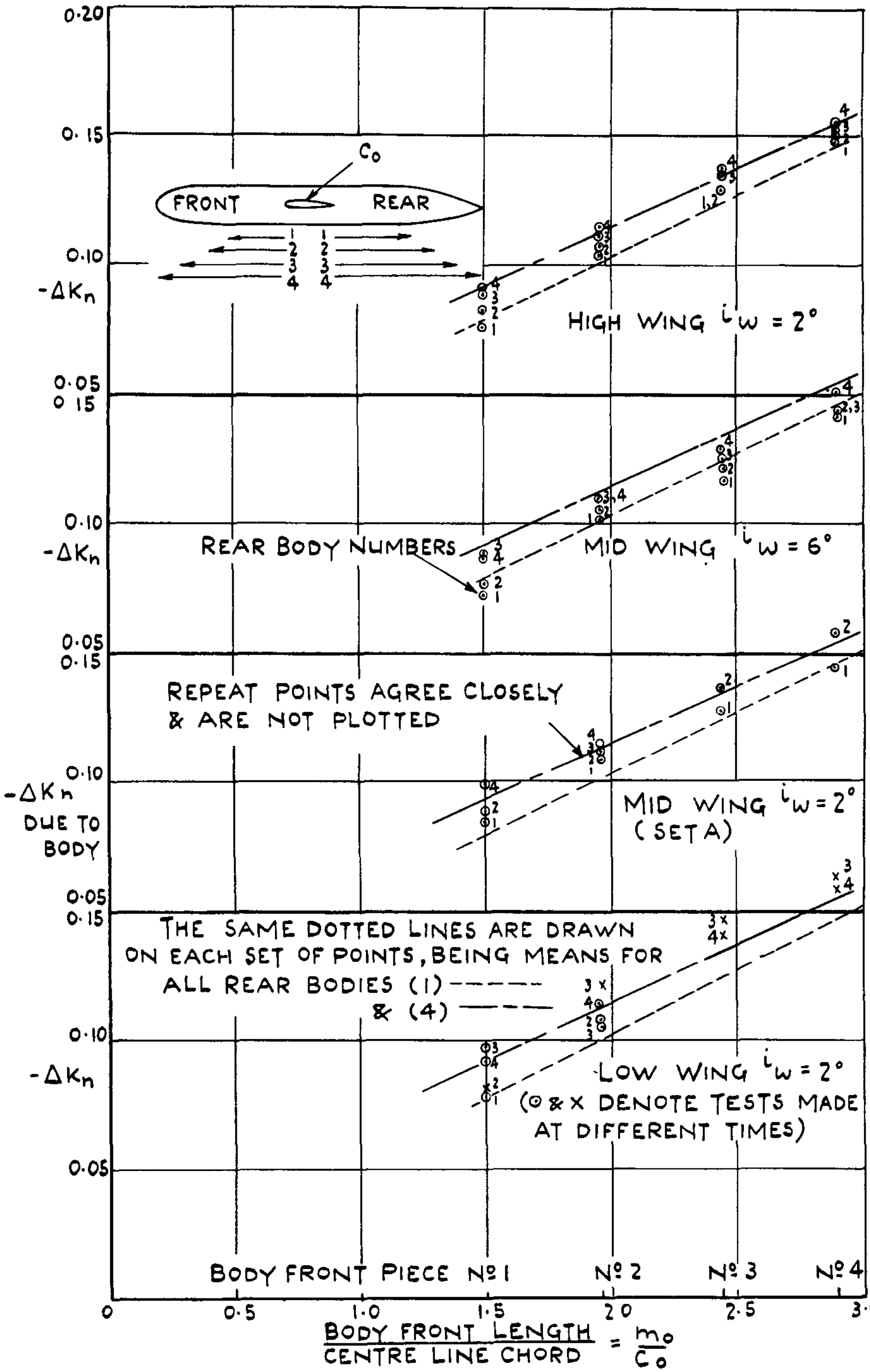

FIG. 8. FORWARD SHIFT OF AERODYNAMIC CENTRE DUE TO BODY ($-\Delta K_n$)

NO FILLETS, 9" DIA: BODY, LARGE SPAN WING

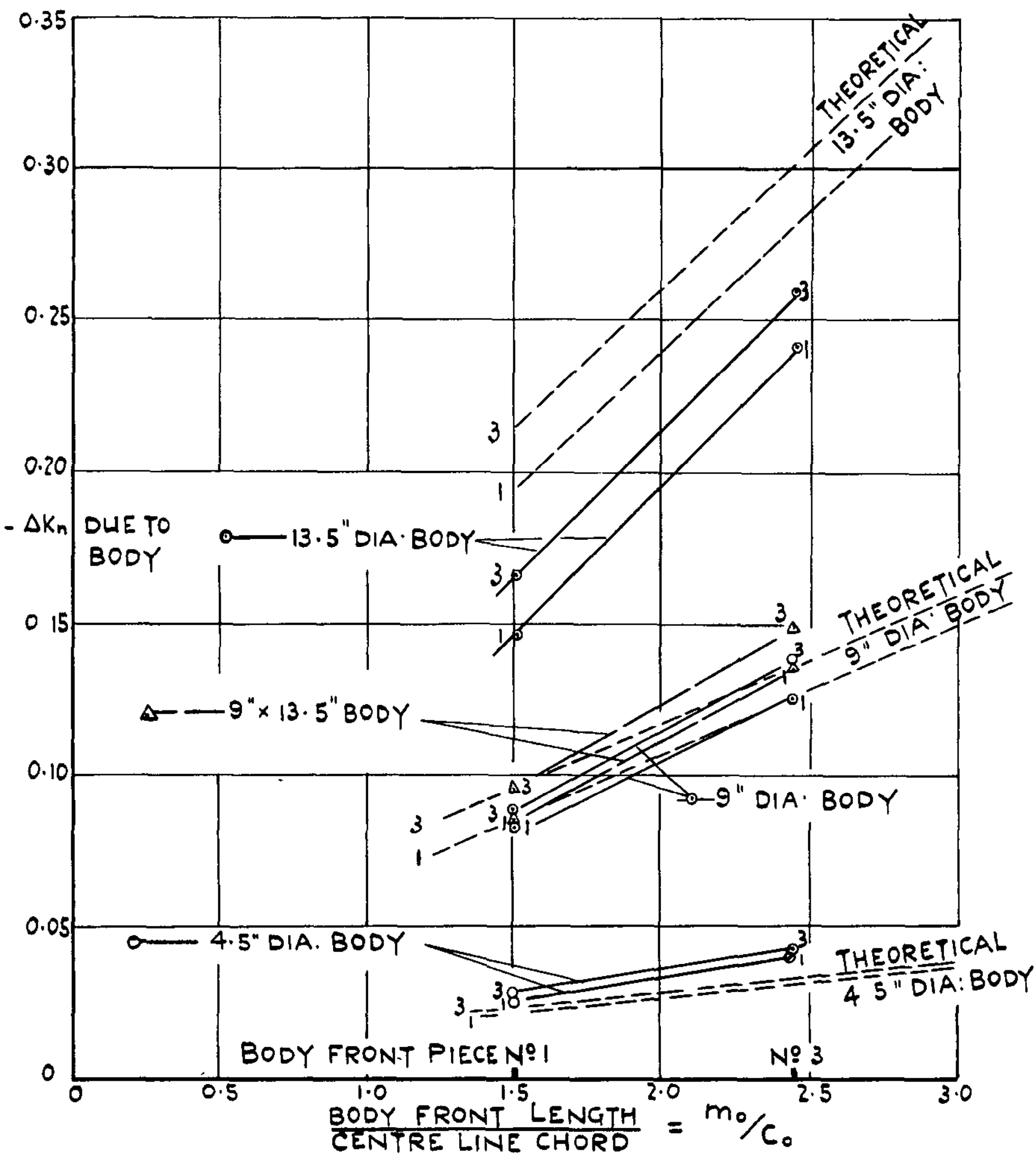

FIG. 9. EFFECT OF BODY DIAMETER AND DEPTH ON $-\Delta K_n$ DUE TO BODY, AND COMPARISON WITH POTENTIAL FLOW THEORY.

LARGE SPAN WING, MID WING, $i_w = 2°$

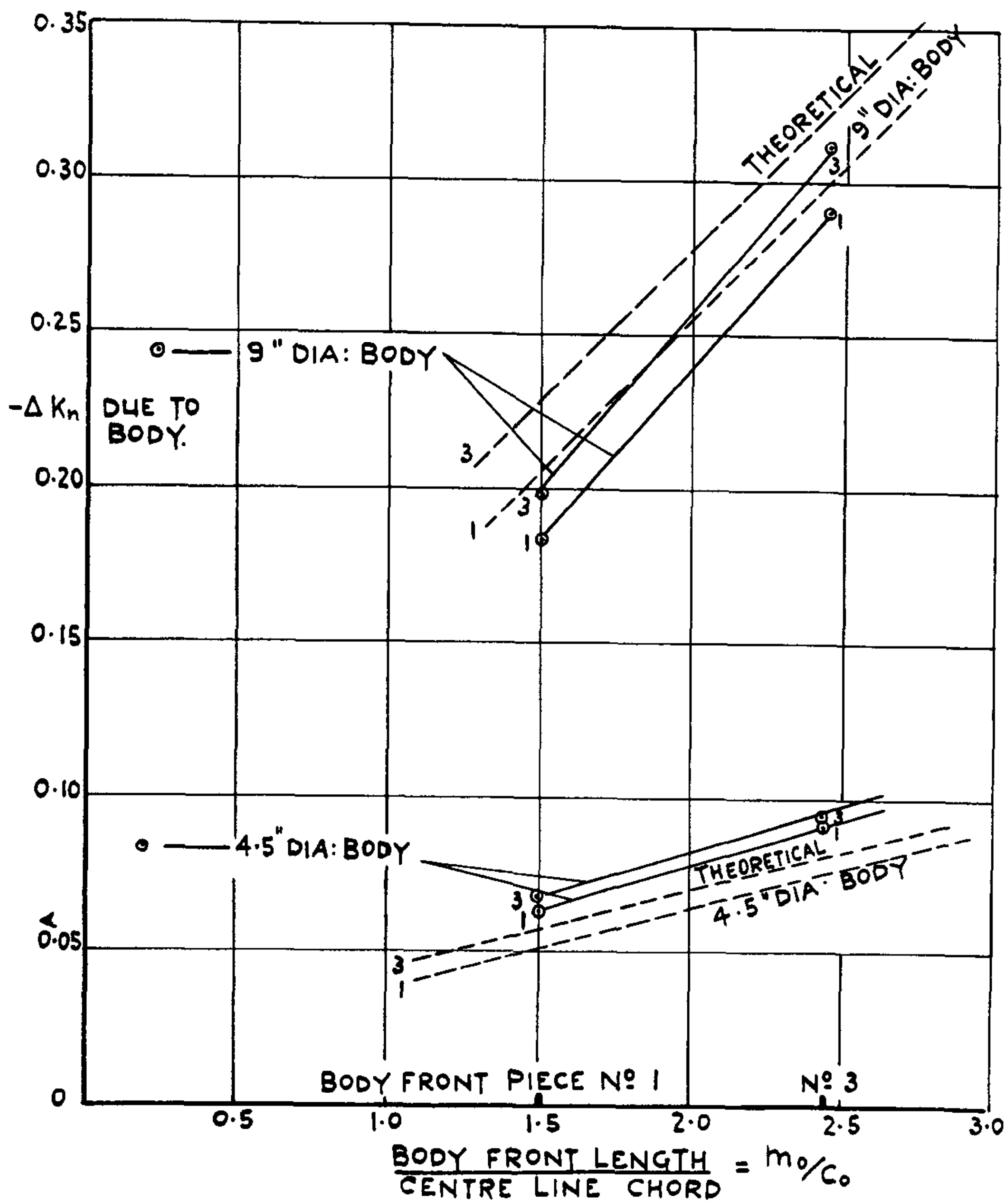

FIG. 10. EFFECT OF BODY SIZE ON $-\Delta K_n$ DUE TO BODY, AND COMPARISON WITH POTENTIAL FLOW THEORY.

SMALL SPAN WING, MID WING, $i_w = 2°$.

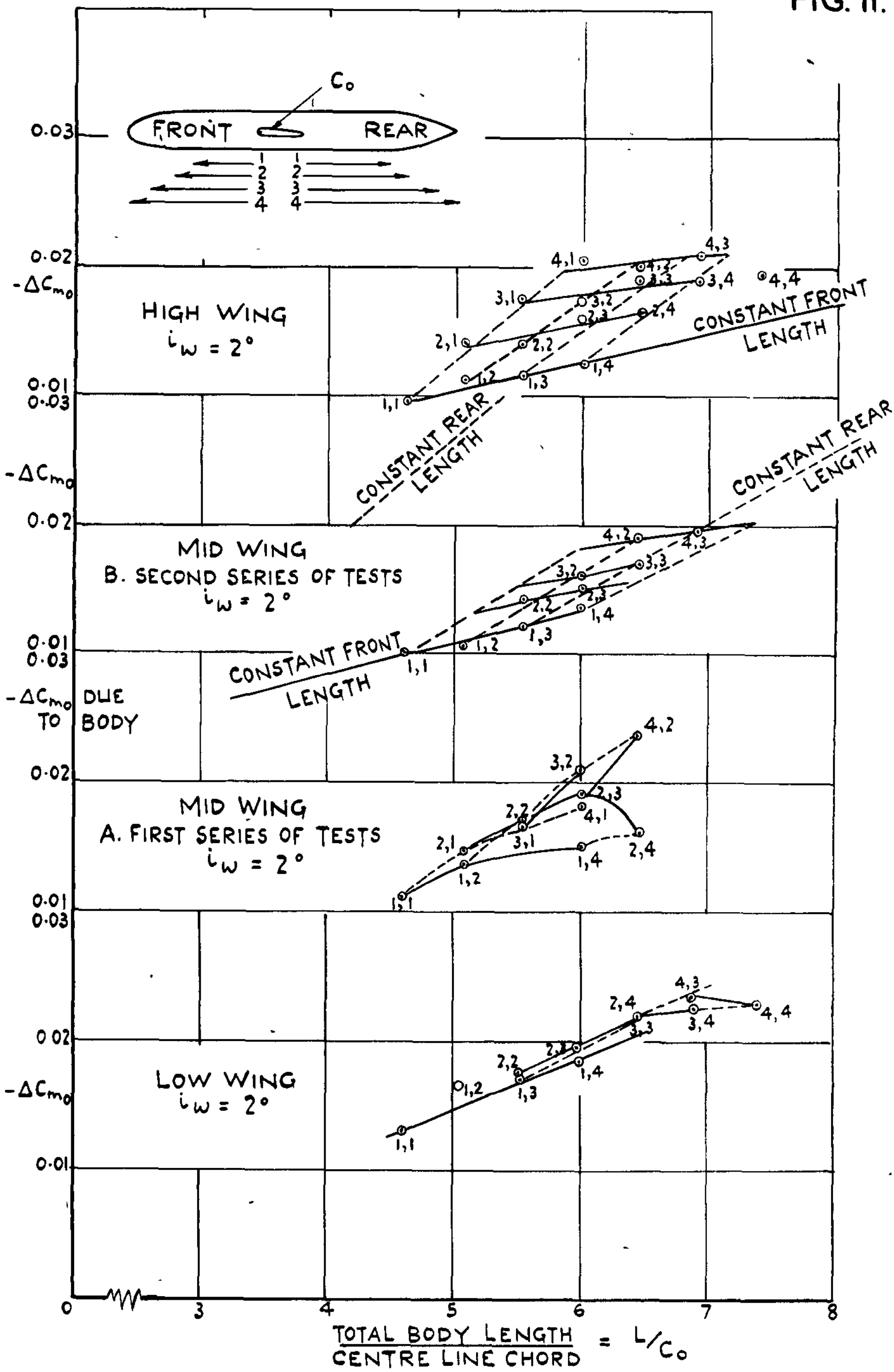

FIG. II. $-\Delta C_{m_0}$ DUE TO BODY.

NO FILLETS, 9" DIA: BODY, LARGE SPAN WING, $i_w = 2°$

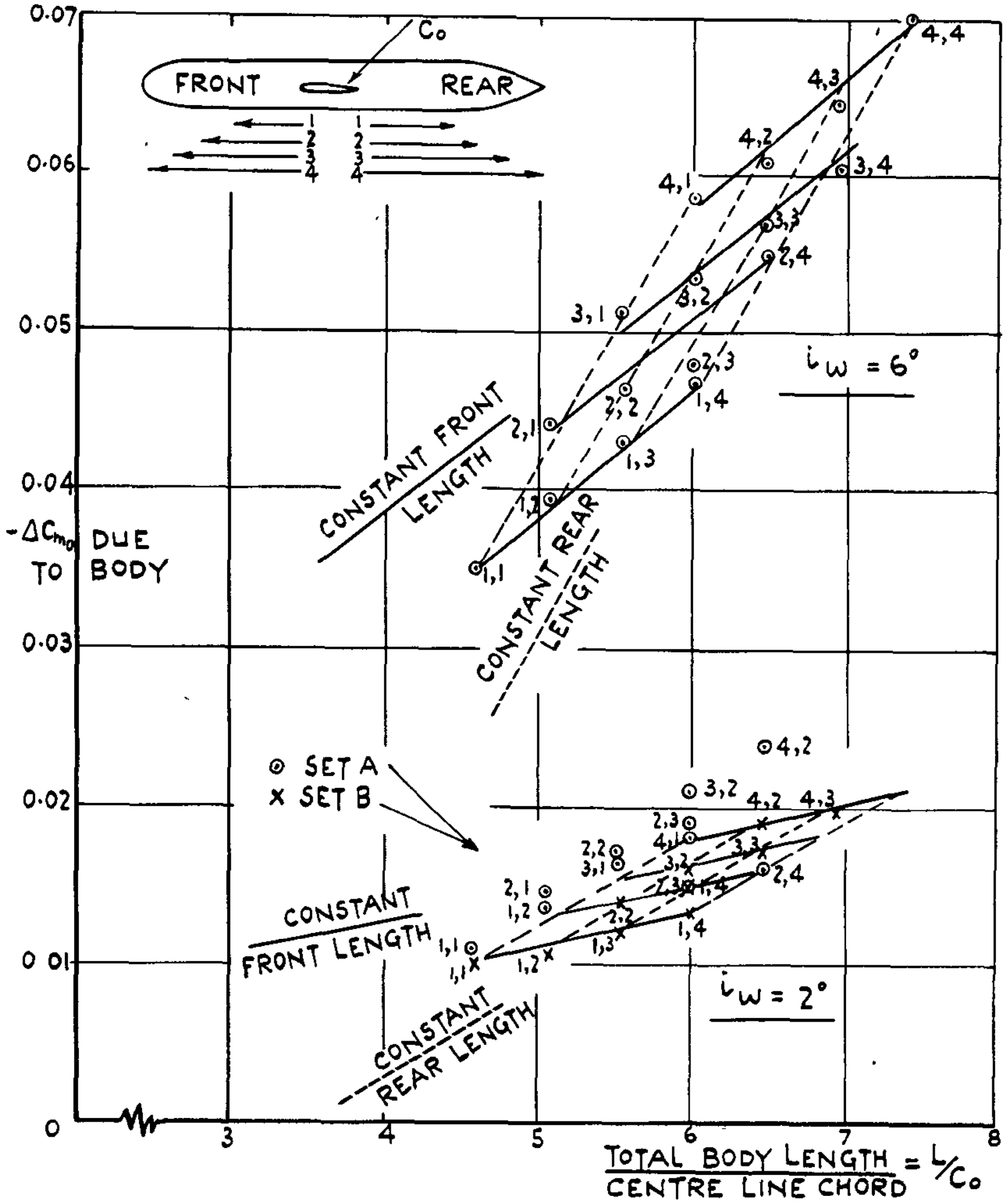

FIG. 12. $-\Delta C_{m_0}$ DUE TO BODY.

MID WING, 9" DIA: BODY, LARGE SPAN WING, $i_w = 2°$ & $i_w = 6°$

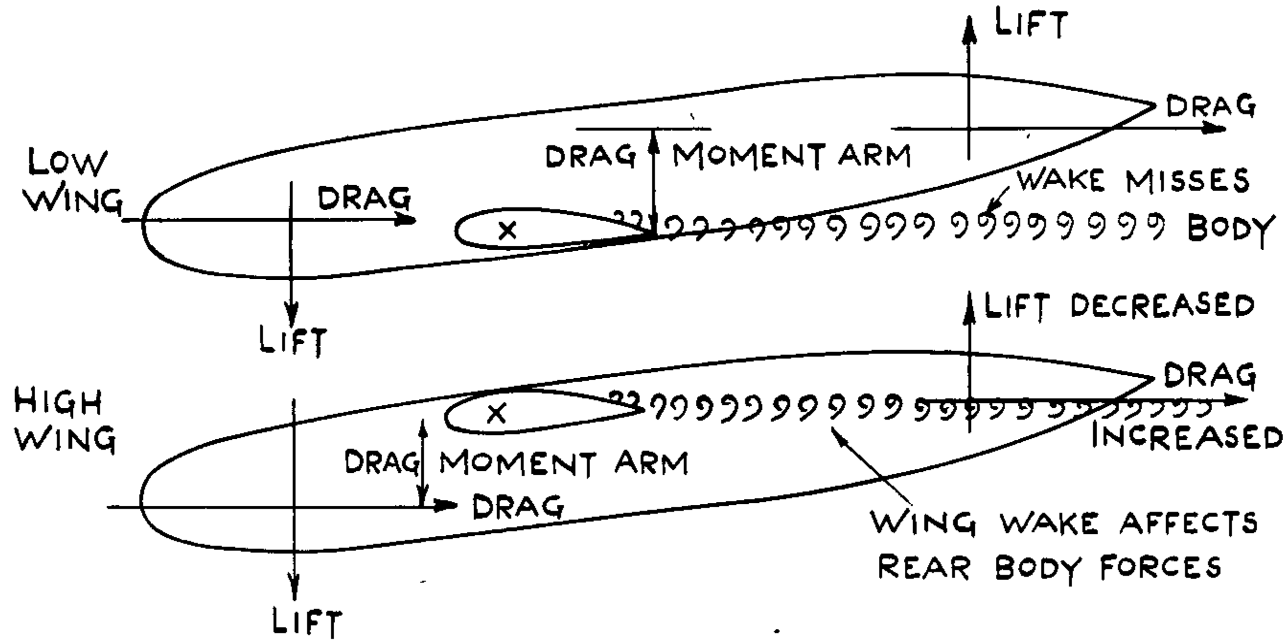

FIG. 13. DIAGRAM OF BODY FORCES AT $C_L = 0$, FOR LOW AND HIGH WING.

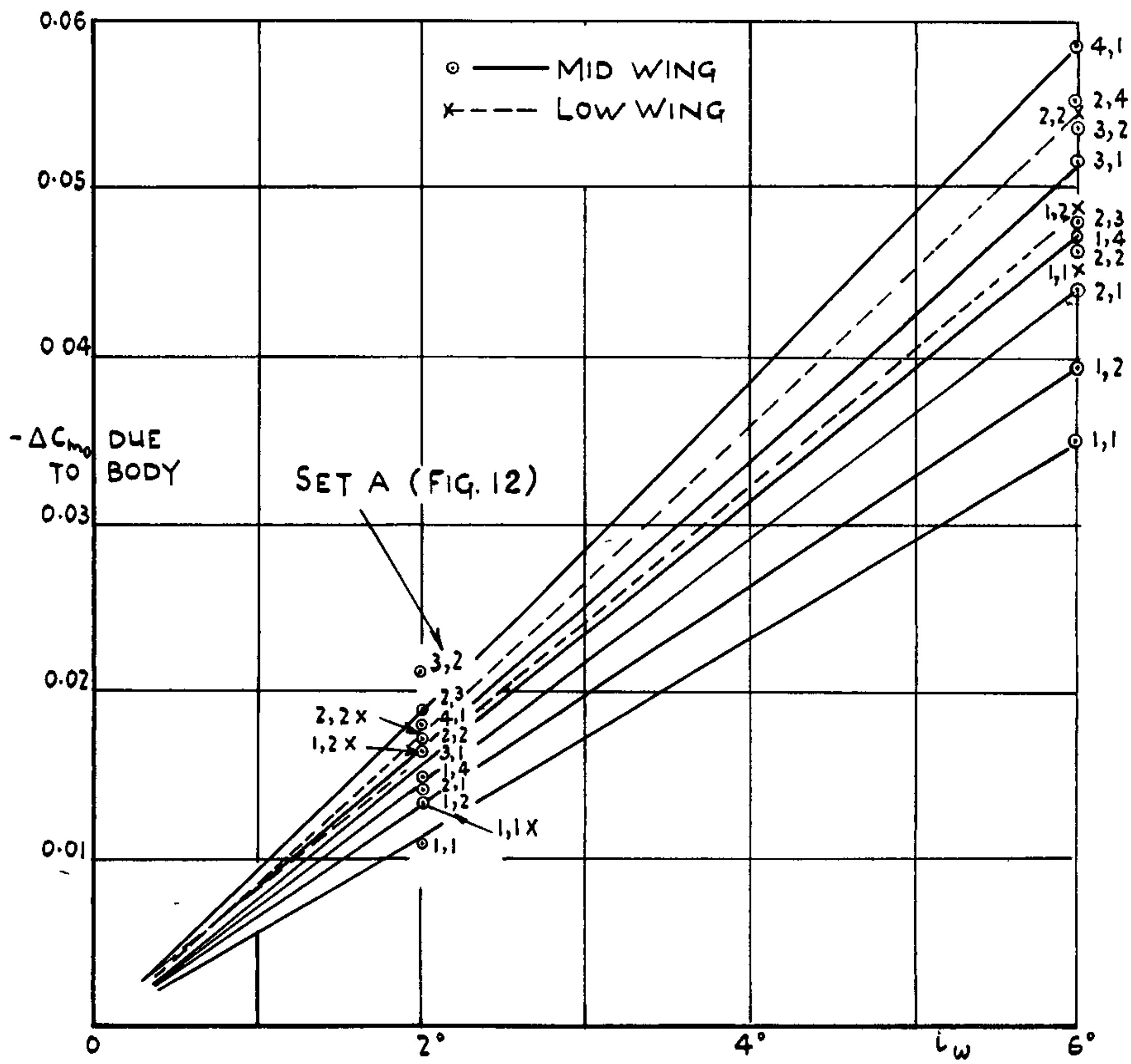

FIG. 14. EFFECT OF i_w ON $-\Delta C_{m_0}$ DUE TO BODY.

NO FILLETS, 9" DIA: BODY, LARGE SPAN WING

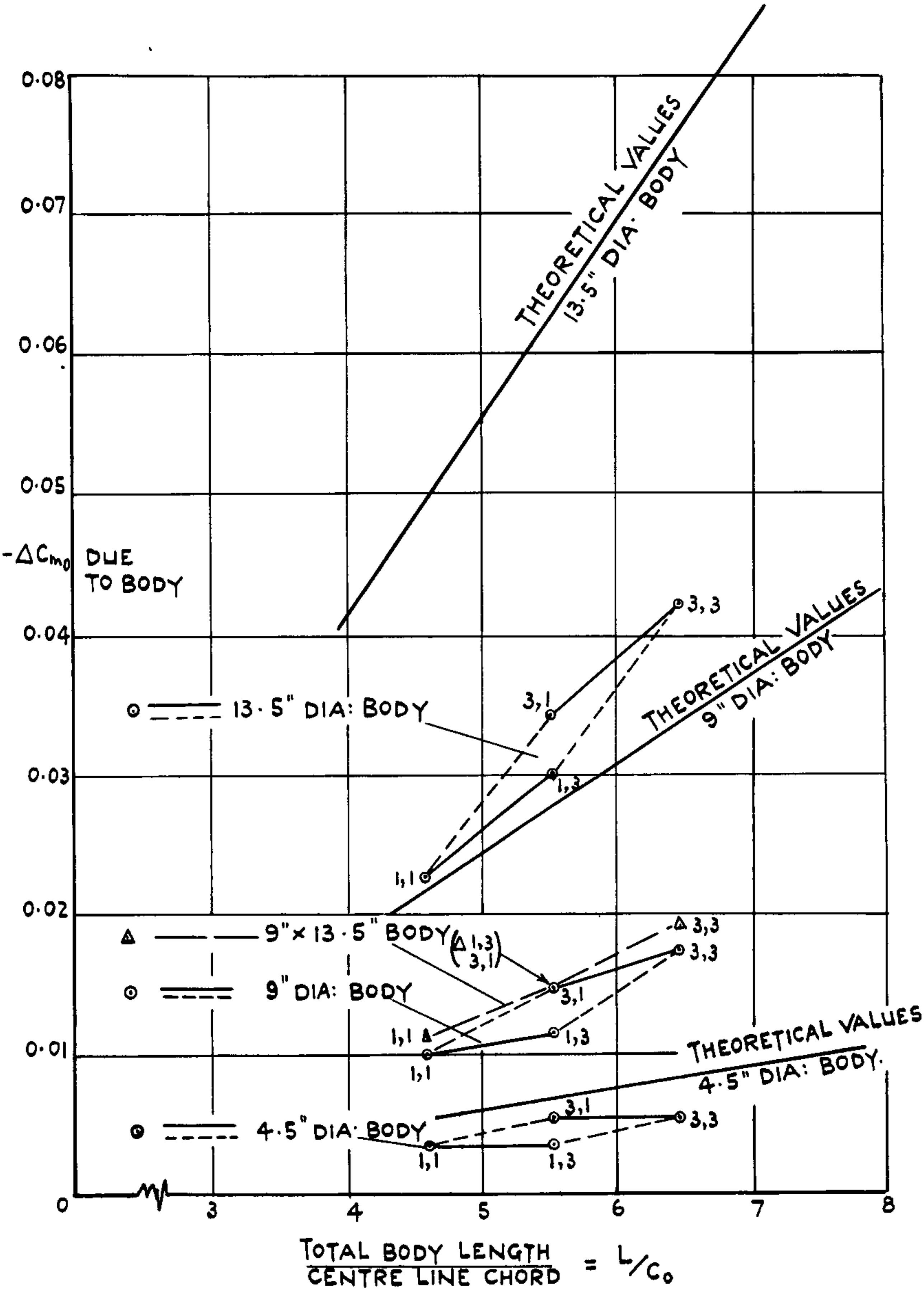

FIG. 15. EFFECT OF BODY DIAMETER AND DEPTH ON ΔC_{m_0} DUE TO BODY, AND COMPARISON WITH POTENTIAL FLOW THEORY.

LARGE SPAN WING, MID WING, $i_W = 2°$

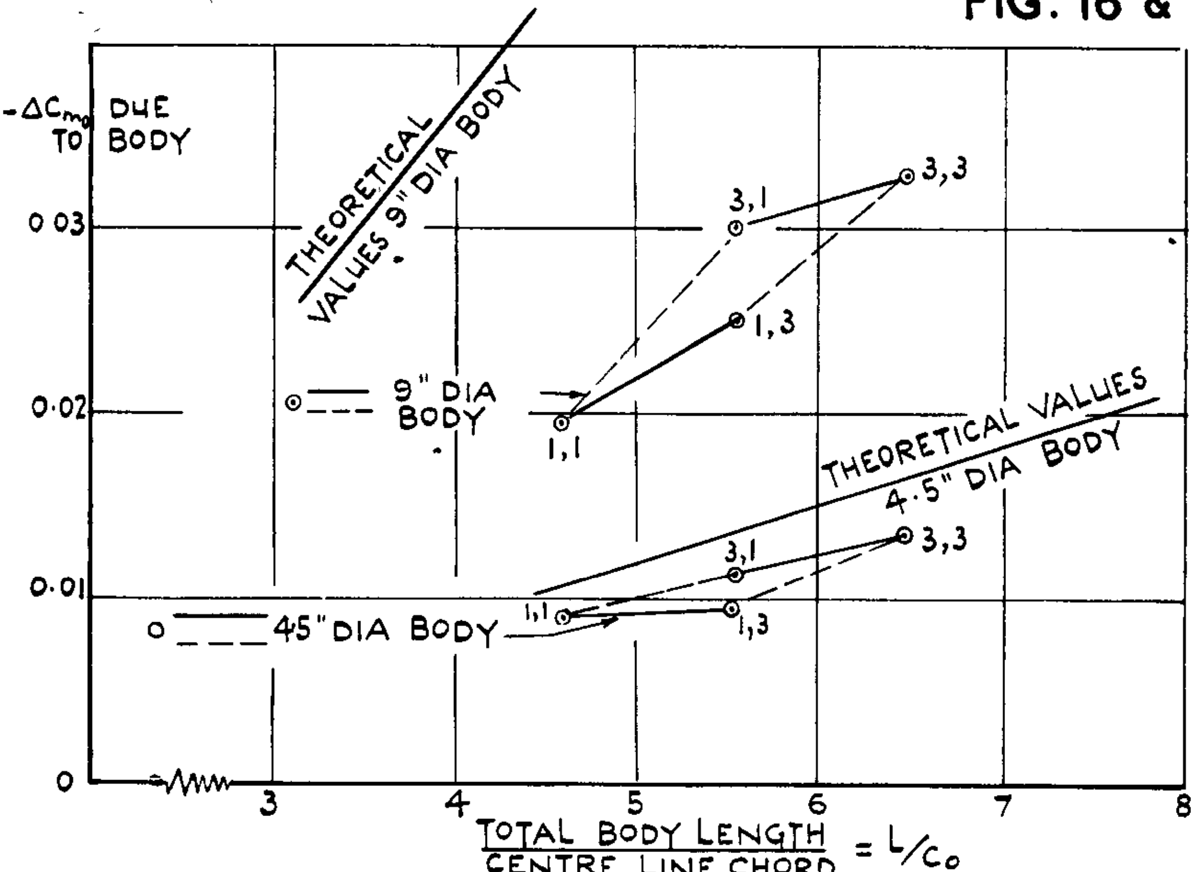

FIG. 16. EFFECT OF BODY DIAMETER ON $-\Delta C_{m_0}$ DUE TO BODY, AND COMPARISON WITH POTENTIAL FLOW THEORY.

SMALL SPAN WING, MID WING, $i_w = 2°$

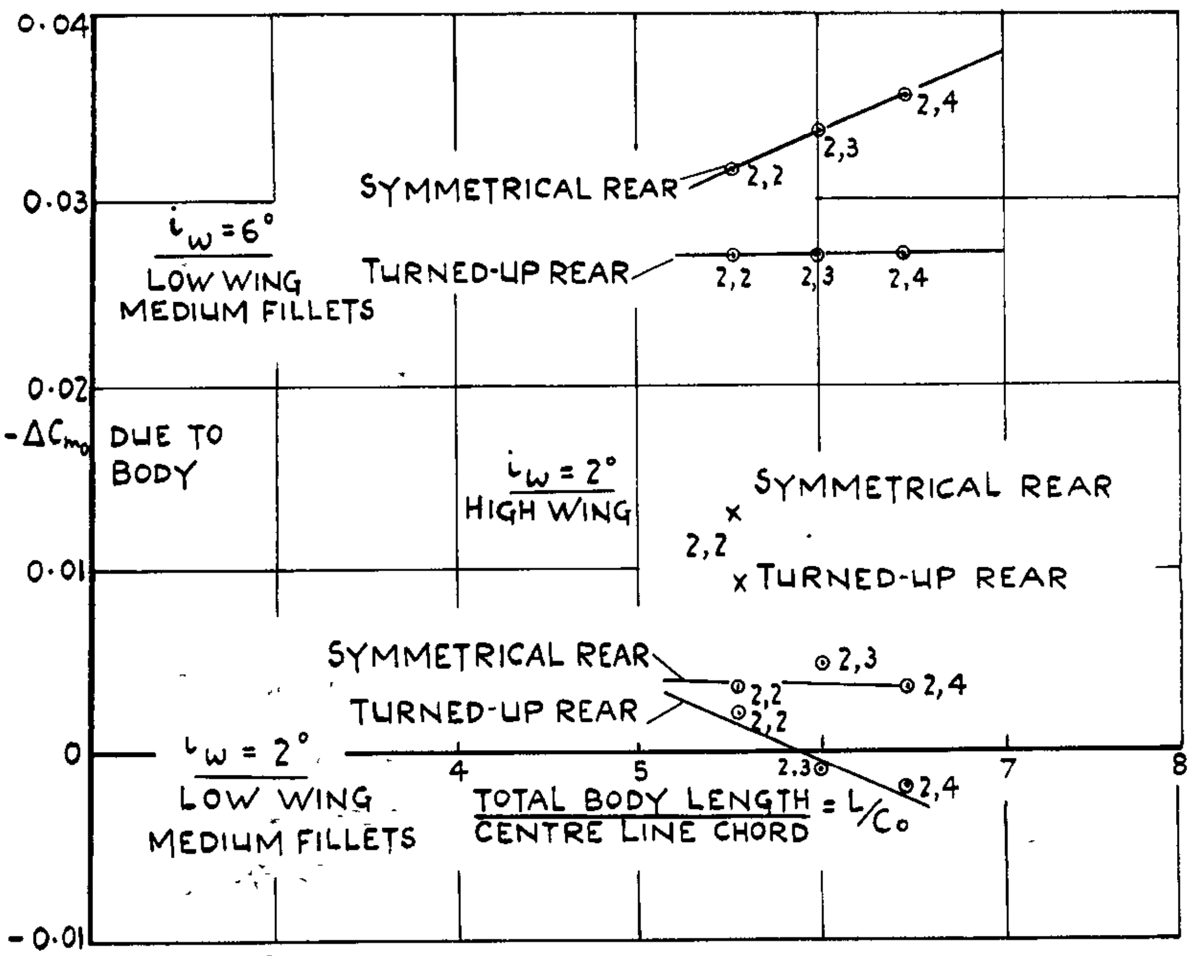

FIG. 17. EFFECT OF TURNED-UP REAR BODY ON $-\Delta C_{m_0}$

9" DIA. BODY, LARGE SPAN WING.

FIG. 18.

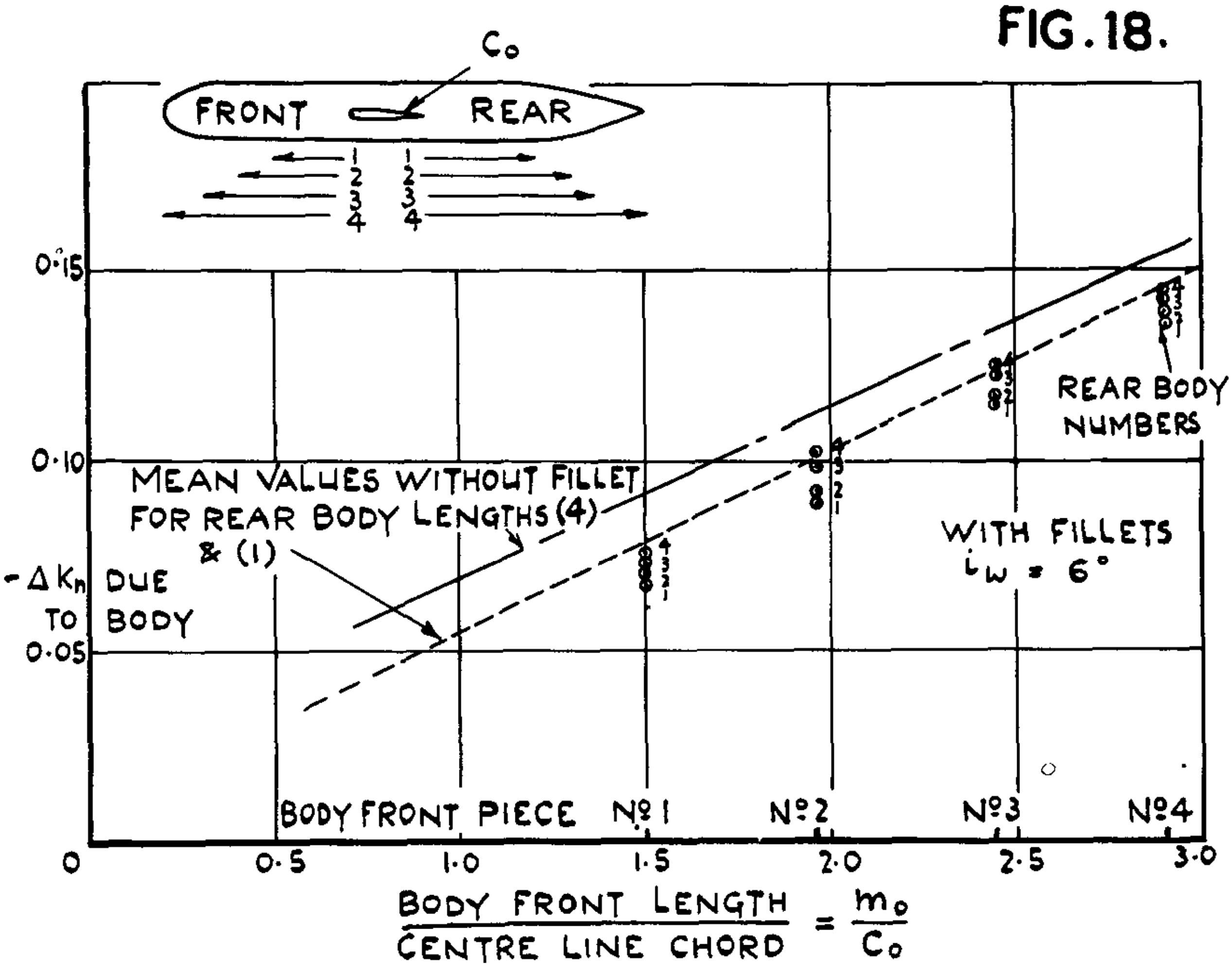

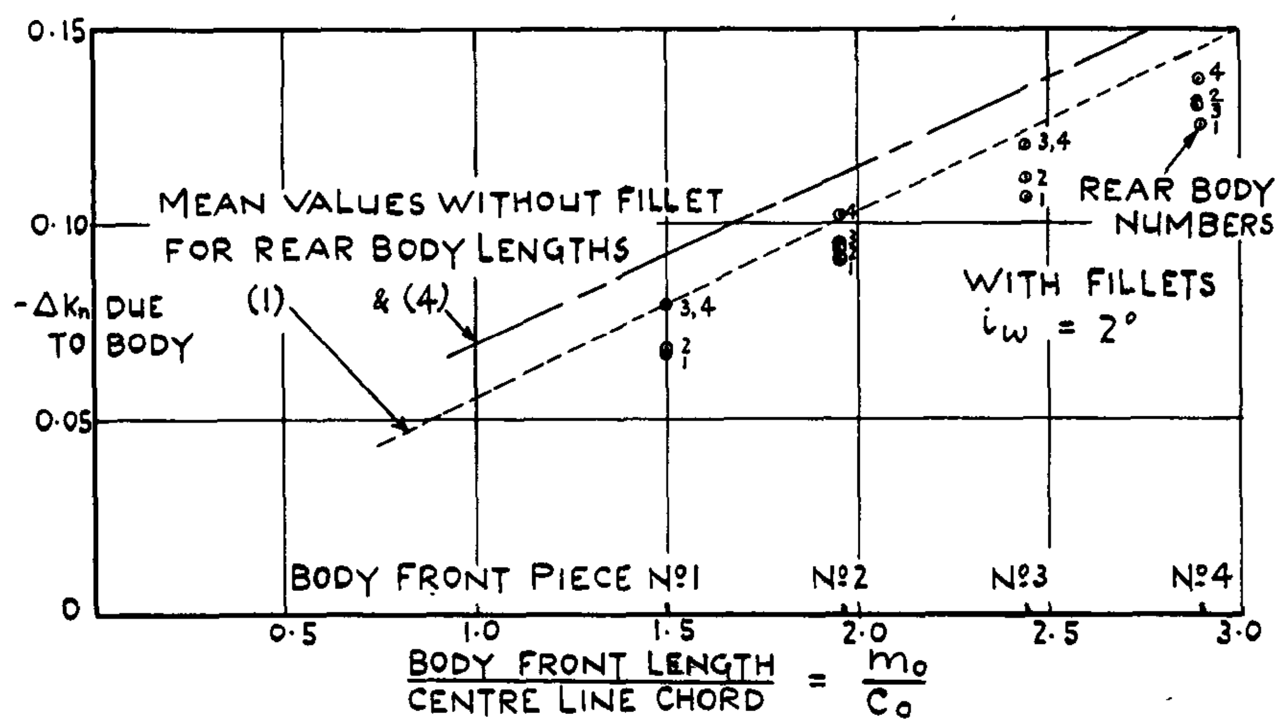

FIG. 18. EFFECT OF FILLETS ON AERODYNAMIC CENTRE.

LOW WING, MEDIUM FILLETS, 9" DIA: BODY, LARGE SPAN WING.
FILLET SHAPE NORMAL, AT 10° TO BODY ($\theta = 12°$ & $16°$)

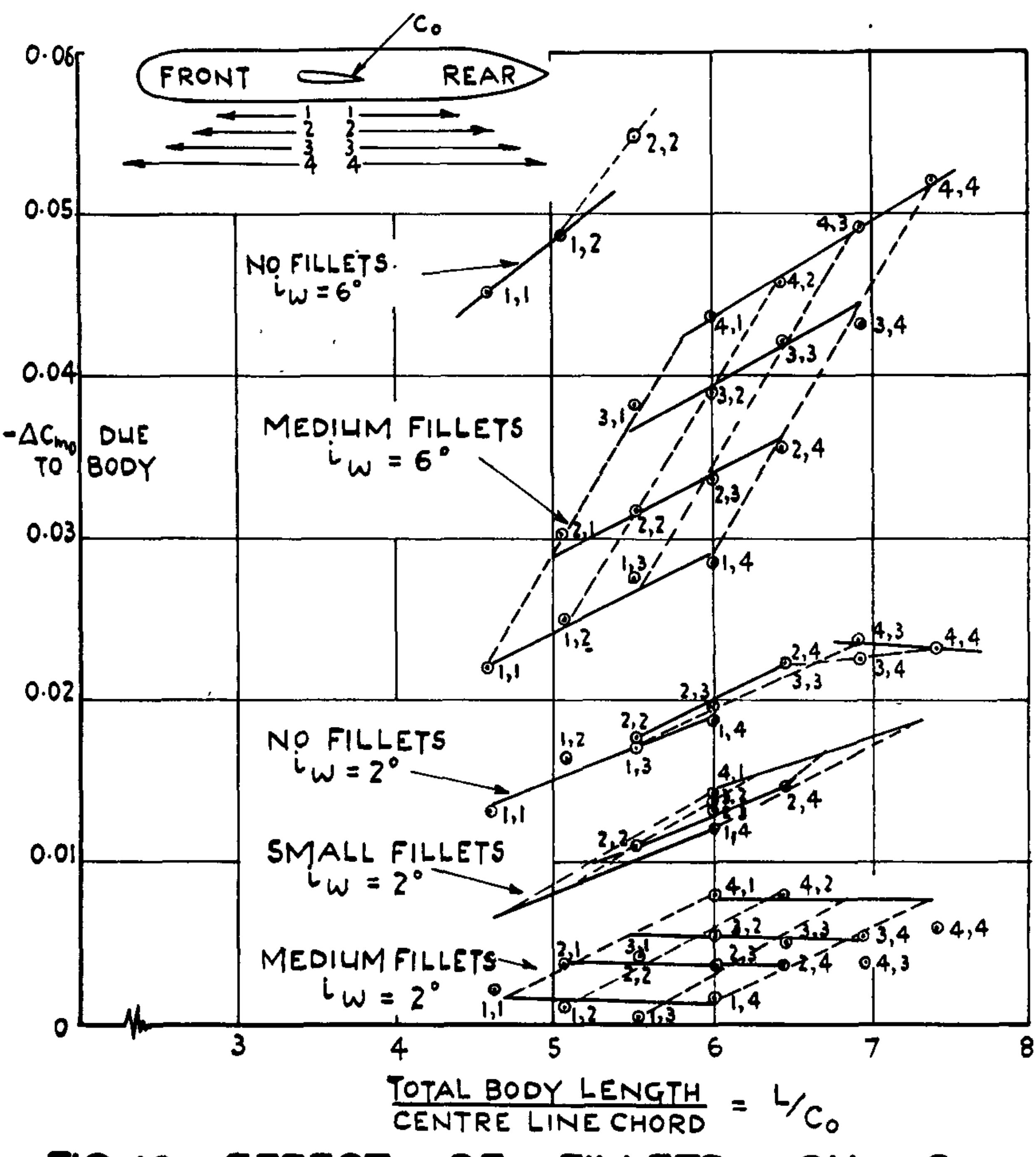

FIG. 19. EFFECT OF FILLETS ON C_{m_0}.

LOW WING, 9" DIA: BODY, LARGE SPAN WING, $\iota_w = 2°$ & $\iota_w = 6°$

FILLET SHAPE NORMAL, AT 10° TO BODY. $\theta = 12°$ & $16°$

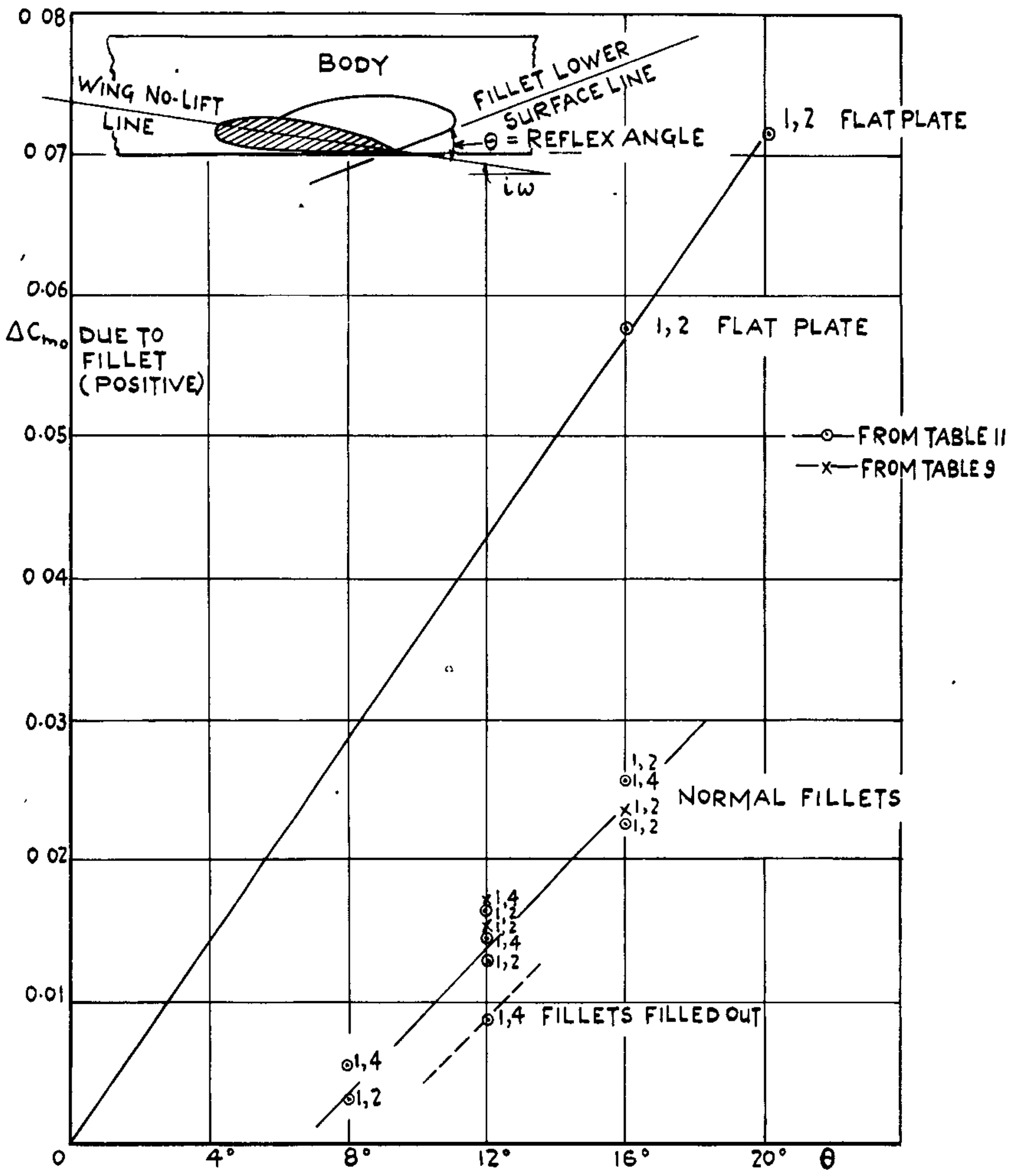

FIG. 20. EFFECT OF FILLET REFLEX, θ, AND THICKNESS ON C_{m_0}

LOW WING, 9" DIA: BODY, LARGE SPAN WING, $i_w = 2°$ & $i_w = 6°$, MEDIUM FILLET PLAN-FORM

FIG. 21.

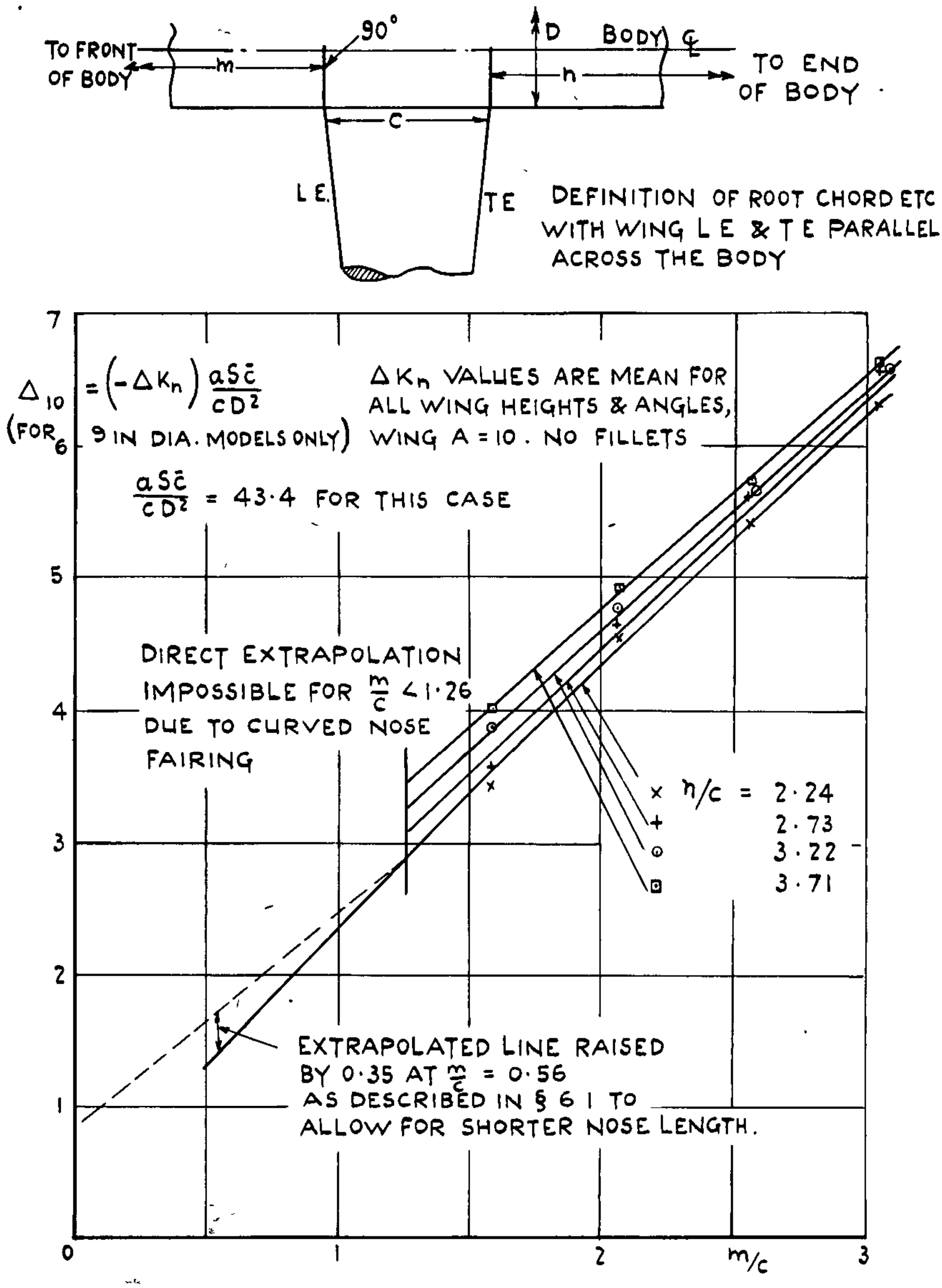

FIG. 21 VALUES OF Δ_{10} FOR 9" DIA: MODEL.

SEE FIG 22 FOR FINAL PRESENTATION

FIG. 22.

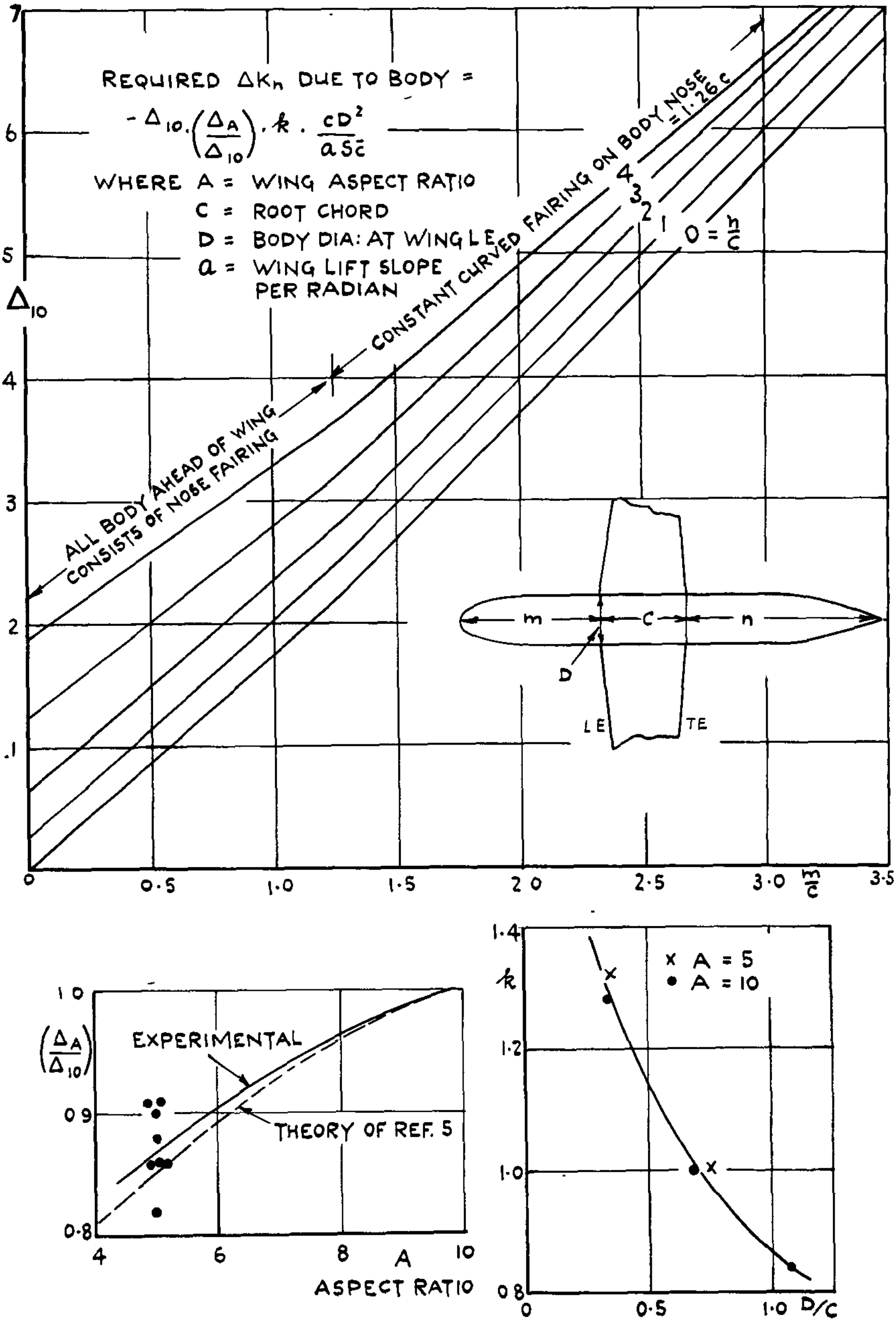

FIG. 22. CHARTS FOR ESTIMATION OF ΔK_n DUE TO BODY.

NO FILLETS, SYMMETRICAL REAR BODY, ELLIPTIC NOSE, BODY OF REVOLUTION ONLY

FIG.23.

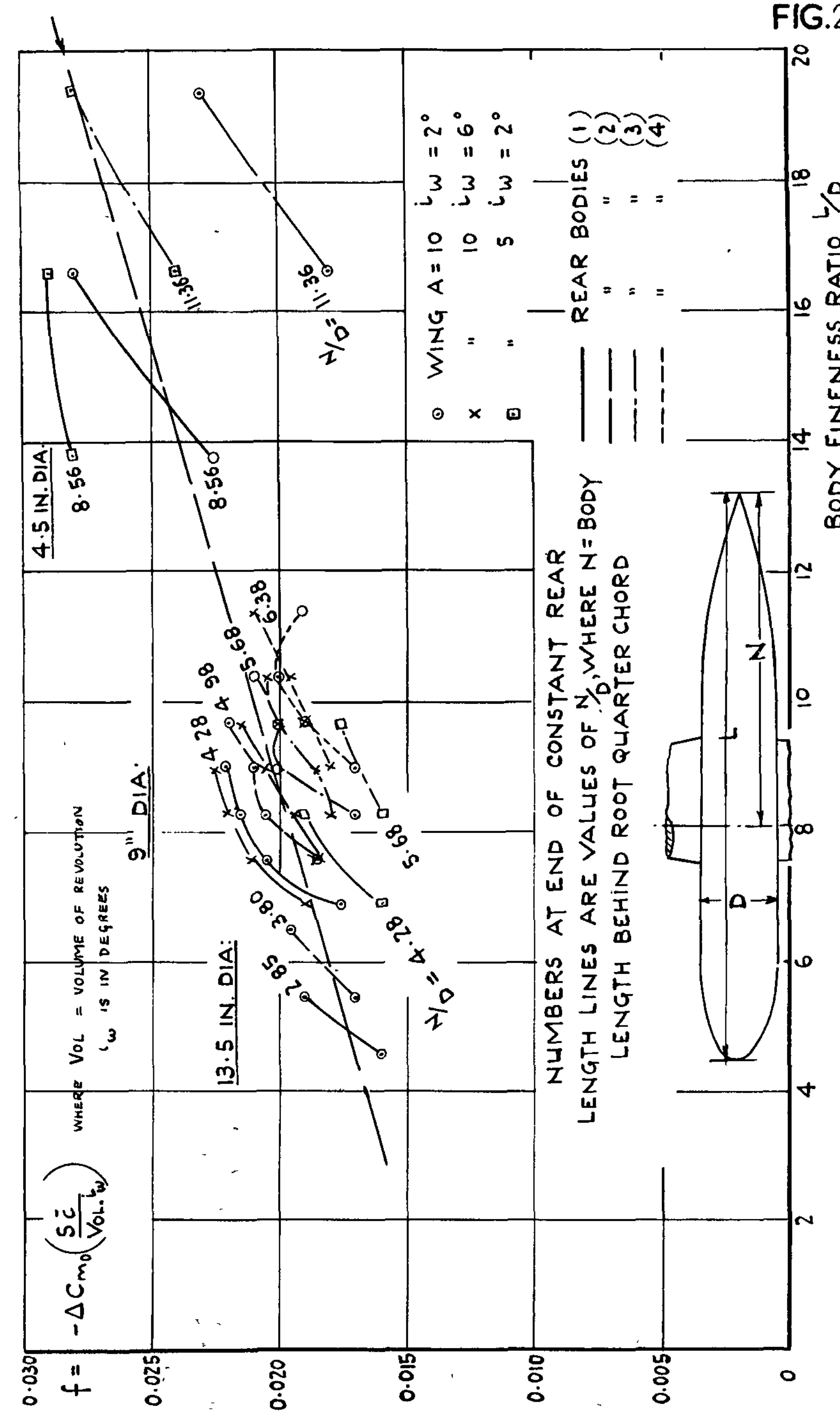

FIG.23. ANALYSIS OF MODEL RESULTS FOR ΔC_{m_0} DUE TO BODY.

BODY OF REVOLUTION ONLY, NO FILLETS.

C.P. No. 16
12492
A.R.C. Technical Report

PUBLISHED BY HIS MAJESTY'S STATIONERY OFFICE
To be purchased from
York House, Kingsway, LONDON, W.C 2, 429 Oxford Street, LONDON, W 1,
P.O. Box 569, LONDON, S.E.1,
13a Castle Street, EDINBURGH, 2 | 1 St Andrew's Crescent, CARDIFF
39 King Street, MANCHESTER, 2 | 1 Tower Lane, BRISTOL, 1
2 Edmund Street, BIRMINGHAM, 3 | 80 Chichester Street, BELFAST,
or from any Bookseller

Price 5s. 6d. net

S.O. Code No. 23 - 9006 - 16